6r. Far Infrared

ERNEST V. LOEWENSTEIN

DONALD R. SMITH

Air Force Cambridge Research Laboratories

6r-1. Sources. Only two broad-band sources are bright enough for use in the far-infrared region. The first is a silicon carbide source of the type used in commercial infrared spectrometers. This source has a temperature of about 1200 K, but transmission measurements indicate that its emissivity decreases at low wave numbers. Therefore, the apparent temperature of such a source decreases with decreasing wave number, and partly for this reason globar sources are rarely if ever used at wave numbers lower than 100 cm^{-1}. The mercury-discharge lamp is the source almost universally used for the far-infrared region. The radiant energy at wave numbers greater than about 140 cm^{-1} comes almost exclusively from the hot envelope. The apparent temperature of this fused-quartz envelope is about 900 to 1200 K [1,2]. Below 140 cm^{-1}, as the envelope becomes progressively more transparent, the radiation from the mercury plasma becomes more important. This radiation follows the same ν^2 wave-number dependence as the envelope emission, but with an effective temperature of the order of 5000 to 7000 K in the central part of the tube [3–6]. Therefore, the apparent temperature of the mercury-lamp source increases rapidly with decreasing wave number below 140 cm^{-1}. The emission of the lamp in this region closely approximates a ν wave-number dependence as observed by McCubbin [7]. Mercury lamps need not be water- or air-cooled, but should be operated with the outer envelope removed since it is highly absorbing in the far infrared, even if it is made of fused quartz. There are many different types of high-pressure mercury-discharge lamps commercially available which are satisfactory as far-infrared sources; the 100-W and 85-W G.E. lamps are the most widely used. Lamps of higher wattage are not, in general, better sources unless a large source area is required.

References for Sec. 6r-1

1. Plyler, E. K., D. J. Yates, and H. A. Gebbie: *J. Opt. Soc. Am.* **52**, 859 (1962).
2. Louden, W. C., and K. Schmidt: *Illum. Engr.* **60**, 696 (1965).
3. Cano, R., and M. Mattioli: *Infrared Phys.* **7**, 25 (1967).
4. Smith, D. R., R. L. Morgan, and E. V. Loewenstein: *J. Opt. Soc. Am.* **58**, 433 (1968).
5. Elenbaas, W.: "The High Pressure Mercury Vapour Discharge," Interscience Publishers, Inc., New York, 1951.
6. Filippov, O. K., and V. M. Pivovarov: *Opt. Spectr.* **16**, 282 (1964).
7. McCubbin, T. King, Jr.: Doctoral Dissertation, The Johns Hopkins University, (1951).

6r-2. Detectors. A large variety of detectors is available for the far infrared, and their characteristics are summarized in Table 6r-1. The room-temperature detectors are slower and less sensitive than the cooled ones, all of which must be cooled to 4.2 K or lower.

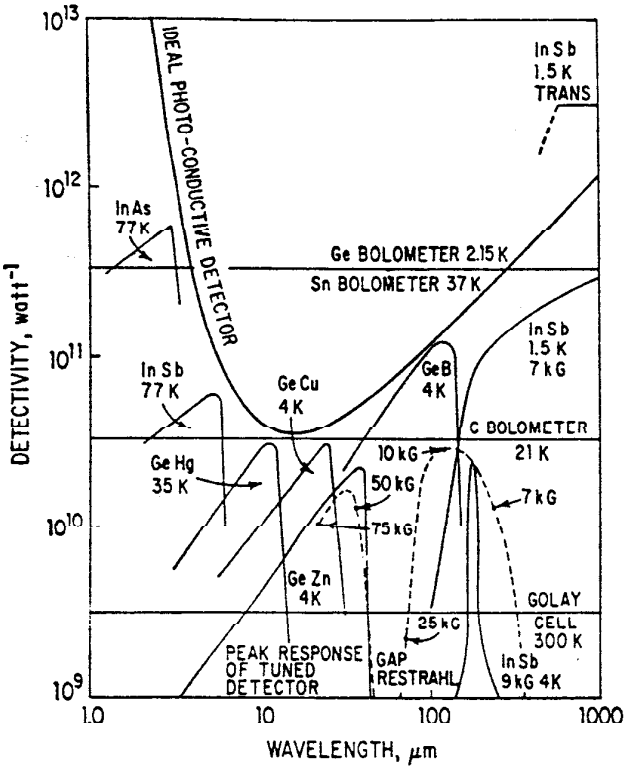

FIG. 6r-1. Performance of far infrared detectors. [Ref. E. Putley, in "Spectroscopic Techniques for Far Infrared and Submillimetre Waves," D. H. Martin, ed., John Wiley & Sons, New York, 1967.]

TABLE 6r-1. CHARACTERISTICS OF FAR-INFRARED DETECTORS

Detector	NEP (for 1 Hz bandwidth), watt	τ sec	Wavelength range	Refs.	Remarks
Golay cell	10^{-10}	10^{-2}	Visible to several mm	1	Room-temperature pneumatic detector
Thermopile	$0.2\text{–}1 \times 10^{-10}$	0.150 in vacuum 0.02 in xenon	Visible to several mm	2	Room temperature
Modified thermistor bolometer	7×10^{-10}	6×10^{-3}	5 μm to 4 mm	3	Room temperature
Carbon bolometer	3×10^{-11}	10^{-3}	Entire infrared	4	<2 K
Germanium bolometer	3×10^{-12}	10^{-3}	1.2 μm to several mm	5, 6	<2 K
InSb (low field)	5×10^{-12}	2×10^{-7}	200 μm to several mm	7, 8	~1.5 K; weak magnetic field
InSb (no field)	3×10^{-13}	10^{-7}	300 μm to several mm	14	~1.8 K; no field, cooled transformer
InSb (high field)	5×10^{-11}	$<10^{-6}$	Tuned, narrow band	7, 8	~4 K; wavelength of peak response, fn. of field
Germanium photoconductor	$\sim 10^{-12}$	10^{-7}	30 to 135 μm	9	~4 K; Ga doped, compensated
Germanium bolometer	3×10^{-14}	10^{-2}	Not given, probably $\lambda\lambda > 100$ μm	15	0.4 K, liquid ^{3}He bath, closed-cycle refrigeration
Silicon bolometer	$\sim 10^{-13}$	$\sim 10^{-3}$	Near IR to several mm	10	1 K; silicon doped with phosphorus and boron
Josephson detector	$\sim 5 \times 10^{-13}$	$<10^{-9}$	See remarks	11	4 K; wavelength range narrow dependent on material used
Superconductor Sn bolometer	10^{-7}	10^{-2}	10 μm to several mm	12	3.7 K
Ga As photoconductor	10^{-13}	$<10^{-6}$	<195 μm to >1 mm	13	4 K

References for Table 6r-1

1. Golay, M. J. E.: *Rev. Sci. Instr.* **20**, 816 (1949).
2. Stafsudd, O., and N. Stevens: *Appl. Opt.* **7**, 2320 (1968).
3. Allen, C., F. Arams, M. Wang, and C. C. Bradley: *Appl. Opt* **8**, 813 (1969).
4. Boyle, W. S., and K. F. Rodgers, Jr.: *J. Opt. Soc. Am.* **49**, 66 (1959).
5. Low, Frank J.: *J. Opt. Soc. Am.* **51**, 1300 (1961).
6. Zwerdling, S., R. A. Smith, and J. P. Theriault: *Infrared Phys.* **8**, 271 (1968).
7. Putley, E.: *J. Sci. Instr.* **43**, 857 (1966).
8. Martin, D. H., ed.: "Spectroscopic Techniques for Far Infrared and Submillimetre Waves," chap. 4. North-Holland Publishing Company, Amsterdam, 1967.
9. Moore, W. J., and H. Shenker: *Infrared Phys.* **5**, 99 (1965).
10. Silvera, I.: Private communication.
11. Grimes, C. C., P. L. Richards, and S. Shapiro: *Phys. Rev. Letters*, **17**, 431 (1966).
12. Martin, D. H., and D. Bloor, *Cryogenics* **1**, 159 (1961).
13. Stillman, G. E., C. M. Wolfe, I. Melngailis, C. D. Parker, P. E. Tannenwald, and J. O. Dimmock: *Appl. Phys. Letters* **13**, 83 (1968).
14. Kinch, M. A., and B. V. Rollin: *Brit. J. Appl. Phys.* **14**, 672 (1963).
15. Drew, H. D., and A. J. Sievers: *App. Opt.* **8**, 2067 (1969).

Most of the detectors are broad-band devices, but some, such as the InSb detector in a magnetic field, are narrow band. The Josephson detector is also a narrow-band detector, and is the fastest and most sensitive yet reported. Difficulties of manufacture are formidable, however, and no general use has been made of this detector.

The material for the germanium and silicon bolometers must be compensated, and no accurate work has been published on the required donor and acceptor concentrations. Ordinarily an ingot of the material is grown, and a search is made for a volume which produces good detectors. Figure 6r-1 gives a graphical comparison of some of the far-infrared detectors.

6r-3. Filters. *Transmission Filters.* The major advantage of transmission filters is that they may be placed anywhere in the optical beam of the instrument. The most widely used filters in the far infrared for the elimination of high-wave-number radiation are absorptive-type transmission filters. These include crystal quartz and black polyethylene, whose transmittance is shown in Figs. 6r-2 and 6r-3. Other materials such as sapphire, fused quartz, and mica can also be used.

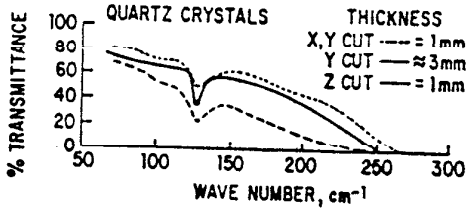

FIG. 6r-2. The transmittance of natural Brazilian crystal quartz. [*From R. V. McKnight and K. D. Möller, J. Opt. Soc. Am.* **54**, 132 (1964).]

Transmission filters with steeper cut-on slopes have been described by Yamada, et al. [1]. They consist of alkali halide crystals suspended in polyethylene and have since come into wide use as low-pass filters for the 400 to 50 cm^{-1} region. By varying the combination of crystal powders used, the cut-on point can be shifted over a wide range of wave numbers. Several of these filters are shown in Fig. 6r-4. If carbon black is mixed with the crystal powders in these filters, the need for a separate black polyethylene filter is eliminated.

Polyethylene filter gratings [2,3] are useful below 50 cm^{-1} where few absorption filters exist. These are constructed by pressing a sheet of polyethylene on a heated metal reflection grating. The position of the transmission minimum is a function of groove shape and spacing; for a symmetric groove of 90-deg apex angle it occurs

at $\lambda/d \approx 0.3$ To give a satisfactory band stop two such filters should be used. T in Fig. 6r-5 represents the transmission for a typical filter. Since these filters work by diffraction, their performance depends upon their location and orientation in the optical beam [3]. Making filter gratings out of black polyethylene eliminates the need for a separate black polyethylene filter.

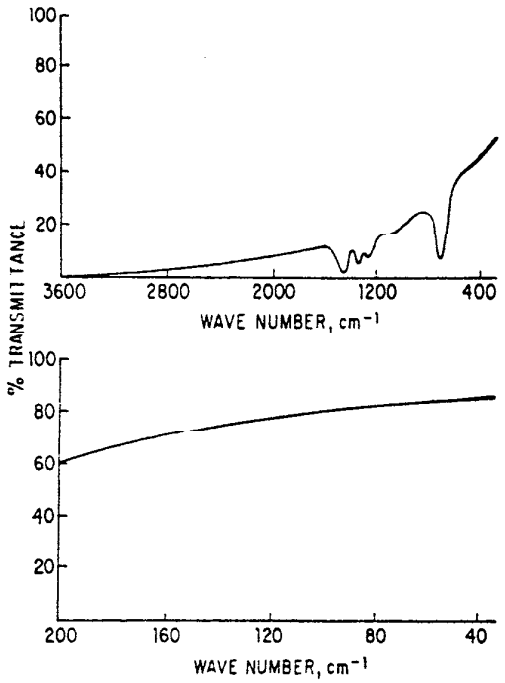

FIG. 6r-3. The transmittance of black polyethylene; thickness, 0.1 mm. [*From K. D. Möller et al., Appl. Opt.* **5**, 403 (1966).]

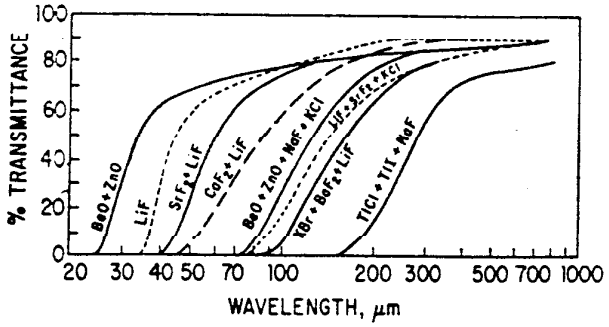

FIG. 6r-4. The transmittance of several typical crystal powder filters. [*From Y. Yamada et al., J. Opt. Soc. Am.* **52**, 17 (1962).]

Thick plates (4.0 to 10.0 mm) of the alkali halide crystals used in the filters described by Yamada et al. are called reststrahlen plates. These are usually single crystals, but plates made of pressed or bonded powders can also be used. In such thicknesses these crystals have extremely strong absorption in the far infrared, but are quite transparent in the near infrared where they are used for prisms and windows. This high-pass characteristic makes these plates useful as chopper blades in far-infrared spectrometers [4]. The chopper used in this manner becomes a low-pass filter since

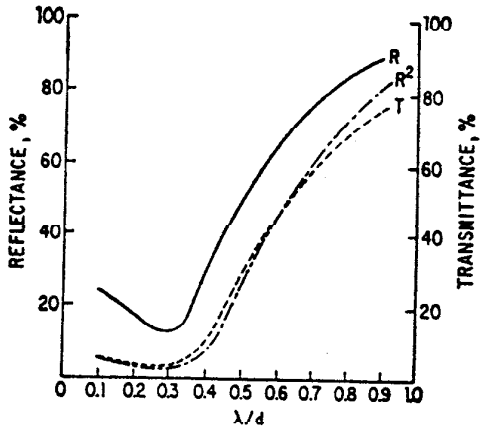

FIG. 6r-5. Comparison of the efficiency of reflection and transmission gratings. R and R^2 represent the characteristics of the reflection from one and two gratings, respectively, and T is the transmittance of a single-transmission filter grating. [*From K. D. Möller and R. V. McKnight, J. Opt. Soc. Am.* **55**, 1075 (1965).]

most of the near-infrared radiation passes unchopped. These plates are also useful for checking the spectral purity of a grating spectrometer. By choosing the proper material and thickness, the first-order radiation of a grating can be eliminated while the overlapping higher orders at shorter wavelengths are allowed to pass. Since only unwanted radiation is recorded, a good estimate of the spectral purity is obtained. The cutoff wave numbers for some typical reststrahlen plates are summarized in Table 6r-2.

TABLE 6r-2. WAVE NUMBERS CORRESPONDING TO A TRANSMITTANCE OF 10% FOR RESTSTRAHLEN CRYSTAL PLATES*

Material	Thickness, mm	Cutoff wave number (10% T)
NaF	10.0	830
BaF_2	9.1	770
NaCl	6.0	490
KCl	5.3	380
KRS-6	6.0	340
KBr	4.0	260
KRS-5	5.1	210
CsBr	5.1	200
CsI	5.0	130

* Data from E. K. Plyler and L. R. Blaine, *J. Res. NBS* **64**, 55 (1960), and S. S. Ballard et al., State-of-the-Art Report: Optical Materials for Infrared Instrumentation, University of Michigan, 1959.

Reflection Filters. Reststrahlen crystals, scatter plates, gratings in the zero order and wire meshes have been employed as reflection filters. They are a rigid part of the optical system, and a filter change must be performed carefully so that the optical alignment is not disturbed. To allow for quick interchanges without the need for realignment, filter-wheel assemblies with three or four positions are generally used, but at a cost of a certain amount of instrument space. Further complications in the

optical path result because two or more reflections are usually necessary to achieve a satisfactory filtering action.

Reststrahlen plates were used as reflection filters by Rubens and others in the earliest experiments in the far infrared. Reflection occurs in the spectral range where these crystals have strong absorption due to lattice vibration. These are basically bandpass filters, but some crystals show low-pass characteristics. Two or more reflections from such crystals are required to achieve adequate attenuation in the band-stop region. The best arrangement is two reflection plates set in crossed positions at the polarizing angle. The performance for a single reflection from such crystals is summarized in Table 6r-3.

TABLE 6r-3. WAVELENGTHS OF THE BAND PEAKS AND THOSE CORRESPONDING TO THE REFLECTIVITY OF 50% FOR VARIOUS RESTSTRAHLEN CRYSTALS*

Reststrahlen crystal	Peak wavelength, μm	Wavelength at 50% level, μm
NaF	34	27 – 42.5
CaF_2	34	21.3 41.2
BaF_2	45	31 – 60
NaCl	53	44.3– 65
KCl	63	54 – 72
KBr	79	68.5 88
KI	92	82 –101
CsBr	122	95 –143
CsI	145	124 –170
TlCl	130	63
TlBr	170	95
KSR-6	155	75
KRS-5	170	112

* From A. Mitsuishi et al., *J. Opt. Soc. Am.* **52**, 14 (1962).

Scatter plates are metal mirrors with an abraded surface which scatter wavelengths shorter than the dimensions of the abrasions in all directions. Such plates ground with carborundum of grades 120, 220, and 320 give cut-on points at about 70, 125, and 180 cm^{-1}, respectively [5,6].

In the case of reflection grating, the wavelengths of interest are reflected in zero order while shorter wavelengths are diffracted out of the beam. Their performance depends on the groove shape and spacing and the angle of incidence of the radiation. Two reflections from such gratings are required to duplicate the performance of a single transmission filter grating and four such reflections to achieve an adequate band-stop attenuation [7,8]. R^2 in Fig. 6r-5 shows the performance of a set of two such filters, while that of a single filter is given by R.

Wire-cloth meshes [9] are the most efficient filters presently in use in the far infrared. These scatter or transmit the unwanted short-wavelength radiation while reflecting the longer wavelengths specularly. Their filter characteristics depend on the wire diameter and spacing as well as on the angle of incidence. The reflectance for five different meshes appears in Fig. 6r-6. In all cases the ratio of the wire diameter to wire spacing was between 0.35 and 0.46 with an angle of incidence of 15 deg. As with other reflection filters, two or more reflections are generally used. The characteristics of the reflectivity of a single mesh and of a set of two and three meshes are

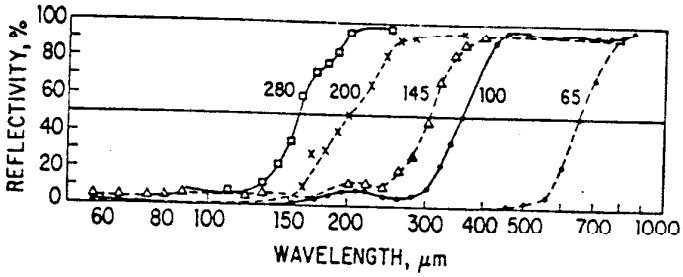

FIG. 6r-6. Reflectance of wire cloth meshes of various mesh number at 15 deg angle of incidence. [*From A. Mitsiushi et al., Japan J. Appl. Phys.* **2**, 574 (1963).]

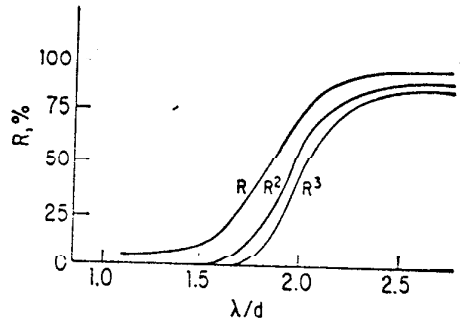

FIG. 6r-7. Reflectance of a typical wire-cloth mesh as a function of λ/d. R, R^2, R^3 represent the effect of one, two, and three reflections, respectively. [*From K. D. Möller et al., J. Opt. Soc. Am.* **55**, 1233 (1965).]

shown in Fig. 6r-7 for a typical mesh. Self-supporting electroformed metallic meshes may also be used as reflection filters, but are not as effective as wire-cloth meshes [10].

Interference Filters. Interference filters for the far infrared making use of the interference between two electroformed metallic meshes have been described by several workers [11–13]. These two-grid filters operating in a high order of interference produce a series of extremely narrow transmission peaks. The complementary structure of metallic meshes for the far infrared was investigated by Ulrich [14]. This complementary structure is made by depositing copper in the form of squares on a Mylar substrate and is referred to as a "capacitive" grid, in contrast to the usual metallic mesh or "inductive" grid. Interference filters consisting of two capacitive

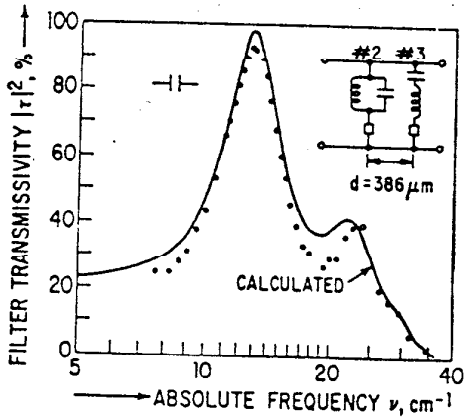

FIG. 6r-8. The transmittance of an interference filter consisting of one inductive and one capacitive grid of grid constant 368 and 250 μm, respectively. The separation of the grids is 386 μm. [*From R. Ulrich, Infrared Phys.* **7**, 37 (1967).]

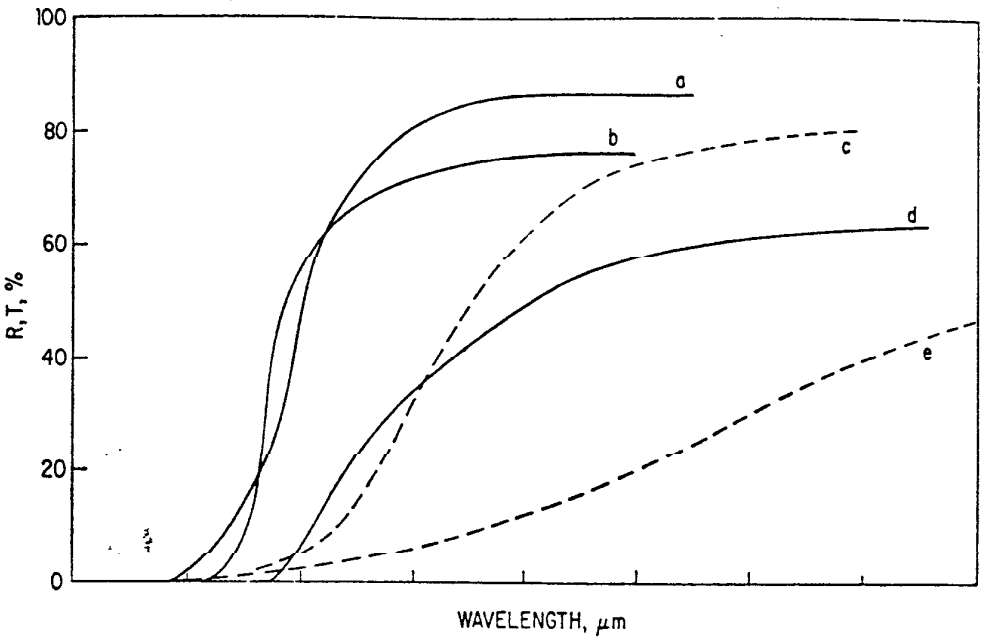

FIG. 6r-9. Characteristics of various reflection and transmission filters. (*a*) Three reflections from a typical wire-cloth mesh. (*b*) A crystal powder filter at 4.2 K containing NaCl, KCl, KBr, KI, CsBr, and CsI. (*c*) A four-grid interference filter of nonidentical grids. (*d*) The same filter as curve *b* at room temperature. (*e*) A set-of-two transmission filter gratings.

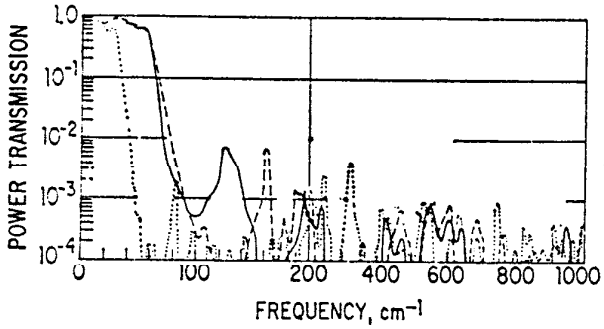

FIG. 6r-10. The transmittance of four-grid filters consisting of capacitive grids of different grid constants. (Grid constants $g_1 = g_2 = g_3 = 102$ μm, $g_4 = 51$ μm, and the spacers $s_1 = s_2 = 50$ μm, $s_3 = 40$ μm. – – – $g_1 = g_4 = 25$ μm, $g_2 = g_3 = 51$ μm, and $s_1 = s_3 = 28$ μm, $s_2 = 20$ μm. – – – – $g_1 = g_4 = 25$ μm, $g_2 = g_3 = 51$ μm, and $s_1 = s_2 = s_3 = 20$ μm.) [*From R. Ulrich, Appl. Opt.* **7**, 1987 (1968).]

grids have characteristics similar to those of the two inductive grid filters except that the finesse increases with frequency. A filter consisting of one inductive and one capacitive grid, however, shows only one interference maximum. One such filter is shown in Fig. 6r-8. In a more recent study Ulrich [15] emphasized the need for using more than two grids to achieve high-performance filters in the far infrared and described multigrid interference filters with low-pass, high-pass, bandpass, and band-stop characteristics. The transmission characteristics of several low-pass filters with extremely wide band stops, steep cut-on slopes, and good attenuation in the band-stop region are given in Fig. 6r-10. These filters consisted of four nonidentical capacitive grids with varied spacers. Although in principle these filters may be scaled to any desired frequency range, in practice they are presently limited to frequencies below 100 cm^{-1}.

Low-temperature Filters. Cooled filters are necessary to minimize heating of a cooled sample under investigation and of the detector itself by radiation from room-temperature surroundings. Cooling increases the cut-on slope and transmittance of many filters. In addition, some materials which are opaque in the far infrared at room temperature become transparent at liquid helium temperature with good transmission characteristics. Many alkali halide crystals [16] and heavily doped silicon [17] are such examples. These filters are usually placed somewhere in the detector dewar for operation at low temperatures. The crystal powder filters described by Yamada et al. show improved performance at low temperatures [18], and crystal quartz, black polyethylene, and sapphire have also been found to be effective filters at these temperatures [19], with improved performance relative to room-temperature operation.

References for Sec. 6r-3

1. Yamada, Y., A. Mitsuishi, and H. Yoshinaga: *J. Opt. Soc. Am.* **52**, 17 (1962).
2. Möller, K. D., and R. V. McKnight: *J. Opt. Soc. Am.* **53**, 760 (1963).
3. Möller, K. D., and R. V. McKnight, *J. Opt. Soc. Am.* **55**, 1075 (1965).
4. Plyler, E. K., and L. R. Blaine: *J. Res. NBS* **64**, 55 (1960).
5. Bloor, D., T. J. Dean, G. O. Jones, D. H. Martin, P. A. Mawer, and C. H. Perry: *Proc. Roy. Soc. (London)*, ser. A, **260**, 510 (1961).
6. Robinson, D. W.: *J. Opt. Soc. Am.* **49**, 966 (1959).
7. White, J. U.: *J. Opt. Soc. Am.* **37**, 713 (1947).
8. Möller, K. D., V. P. Tomaselli, L. R. Skube and B. K. McKenna: *J. Opt. Soc. Am.* **55**, 1233 (1965).
9. Mitsuishi, A., Y. Otsuka, S. Fujita, and H. Yoshinaga: *Japan. J. Appl. Phys.* **2**, 574 (1963).
10. Ressler, G. M., and K. D. Möller: *Appl. Opt.* **6**, 893 (1967).
11. Rawcliffe, R. D., and C. M. Randall: *Appl. Opt.* **6**, 1353 (1967).
12. Ulrich, R., K. F. Renk, and L. Genzel: *IEEE Trans. on MTT* **11**, 363 (1963).
13. Renk, K. F., and L. Genzel: *Appl. Opt.* **1**, 643 (1962).
14. Ulrich, R.: *Infrared Phys.* **7**, 37 (1937).
15. Ulrich, R.: *Appl. Opt.* **7**, 1987 (1968).
16. Hadni, A., J. Claudel, X. Gerbaux, G. Morlot, and J. M. Munier: *Appl. Opt.* **4**, 487 (1965).
17. Neuringer, L. J., and R. C. Milward: *Appl. Opt.* **6**, 978 (1967).
18. Zwerdling, S., and J. P. Theriault: *Appl. Opt.* **7**, 209 (1968).
19. Wheeler, R. G., and J. C. Hill: *J. Opt. Soc. Am.* **56**, 657 (1966).

6r-4. Calibration. The pure rotation spectra of simple gases can be used to calibrate the far-infrared region. A number of such gases and the regions in which they are useful for calibration are given in Table 6r-4. The wave numbers of the rotational lines for each gas appear in Tables 6r-5 to 6r-8. Calibration can also be accomplished by using the higher orders of diffraction of a strong visible or near-infrared line, such as the mercury green line or a laser line.

TABLE 6r-4. CALIBRATION GASES FOR THE FAR-INFRARED REGION

Calibration gas	Useful calibration region, cm^{-1}	Number of lines	Dipole moment,* debyes	Average spacing, cm^{-1}	J_{max}
H_2O	18–400	~250	1.85	Irregular	
CO	4–120	30	0.112	3.8	7
HCN	3–120	40	2.98	2.9	8
N_2O	1– 40	60	0.167	0.8	15
CH_3Cl	1– 40	45	1.87	0.9	14
HCl	20–300	15	1.08	20.9	3

* From R. D. Nelson, Jr. et al., *Selected Values of Electric Dipole Moments for Molecules in the Gas Phase, National Bureau of Standards Report NSRDS-NBS* 10 (September 1967).

TABLE 6r-5. CALCULATED WAVE NUMBERS OF THE PURE ROTATIONAL SPECTRUM OF CO, HCN, N_2O MOLECULES*

J	$C^{12}O^{16}$	$N_2^{14}O^{16}$	$HC^{12}N^{14}$	J	$C^{12}O^{16}$	$N_2^{14}O^{16}$	$HC^{12}N^{14}$
0	3.84_5	0.83_8	2.95_6	25	99.54_1	21.77_6	76.66_3
1	7.69_0	1.67_6	5.91_3	26	103.33_4	22.61_3	79.59_5
2	11.53_4	2.51_4	8.86_9	27	107.12_4	23.44_9	82.52_4
3	15.37_9	3.35_2	11.82_5	28	110.90_9	24.28_5	85.45_3
4	19.22_2	4.19_0	14.78_1	29	114.69_0	25.12_2	88.37_9
5	23.05_5	5.02_8	17.73_6	30	118.46_7	25.95_8	91.30
6	26.90_7	5.86_6	20.69_1	31		26.79_4	94.22
7	30.74_8	6.70_4	23.64_6	32		27.62_9	97.14
8	34.58_8	7.54_2	26.59_9	33		28.46_5	100.06
9	38.42_6	8.38_0	29.55_3	34		29.30_1	102.98
10	42.26_3	9.21_7	32.50_5	35		30.13_6	105.89
11	46.09_8	10.05_5	35.45_7	36		30.97_1	108.80
12	49.93_2	10.89_3	38.40_8	37		31.80_6	111.71
13	53.76_3	11.73_0	41.35_8	38		32.64_1	114.61
14	57.59_3	12.56_8	44.30_7	39		33.47_6	117.51
15	61.42_0	13.40_5	47.25_5	40		34.31_0	120.41
16	65.24_5	14.24_3	50.20_2	41		35.14_5	
17	69.06_8	15.08_0	53.14_8	42		35.97_9	
18	72.88_8	15.91_8	56.09_2	43		36.81_3	
19	76.70_5	16.75_5	59.03_4	44		37.64_7	
20	80.51_9	17.59_2	61.97_7	45		38.48_1	
21	84.33_0	18.42_9	64.91_8	46		39.31_4	
22	88.13_8	19.26_6	67.85_6	47		40.14_7	
23	91.94_3	20.10_3	70.79_3	48		40.98_0	
24	95.74_4	20.94_0	73.72_9	49		41.81_3	
				50		42.64_6	

* From K. N. Rao et al., *J. Res. NBS* 67A, 351 (1963).
Path length 40 cm at pressures 2 to 3 cm of Hg for HCN, and 40 to 60 cm of Hg for CO and N_2O.

TABLE 6r-6. CALCULATED WAVE NUMBERS OF THE PURE ROTATIONAL SPECTRUM OF METHYL CHLORIDE*

$\nu = 2B(J+1) - 4D(J+1)^3$

J	CH_3Cl^{35} $2B = 0.8868\ cm^{-1}$ $4D = 2.4 \cdot 10^{-6}\ cm^{-1}$ ν, cm^{-1}	CH_3Cl^{37} $2B = 0.8731\ cm^{-1}$ $4D = 3.6 \cdot 10^{-6}\ cm^{-1}$ ν, cm^{-1}	J	CH_3Cl^{35} $2B = 0.8868\ cm^{-1}$ $4D = 2.4 \cdot 10^{-6}\ cm^{-1}$ ν, cm^{-1}	CH_3Cl^{37} $2B = 0.8731\ cm^{-1}$ $4D = 3.6 \cdot 10^{-6}\ cm^{-1}$ ν, cm^{-1}
0	0.886_8	0.8731	11	10.6_4	10.47
1	1.77_4	1.746	12	11.52	11.34
2	2.660	2.619	13	12.4_1	12.21
3	3.547	3.492	14	13.29	13.0_9
4	4.43_4	4.365	15	14.1_8	13.9_4
5	5.320	5.238	16	15.06	14.8_8
6	6.207	6.11_1	17	15.9_5	15.7_0
7	7.093	6.983	18	16.83	16.5_7
8	7.979	7.85_6	19	17.7_2	17.43
9	8.86_6	8.72_8	20	18.60	18.30
10	9.75_2	9.60_0			

* From K. D. Möller et al., *J. Opt. Soc. Am.* **55**, 1233 (1965).

TABLE 6r-7. CALCULATED WAVE NUMBERS OF THE PURE ROTATIONAL SPECTRUM OF HYDROGEN CHLORIDE*

$J'' \rightarrow J'$	HCl^{35}	HCl^{37}	$J'' \rightarrow J'$	HCl^{35}	HCl^{37}
$0 \rightarrow 1$	20.878_2	20.846_8	$8 \rightarrow 9$	186.38_7	186.10_8
$1 \rightarrow 2$	41.743_7	41.681_0	$9 \rightarrow 10$	206.69_8	206.38_8
$2 \rightarrow 3$	65.583_9	62.489_9	$10 \rightarrow 11$	226.88_8	226.54_2
$3 \rightarrow 4$	83.386_1	83.260_8	$11 \rightarrow 12$	246.93_0	246.56_0
$4 \rightarrow 5$	104.137_7	103.981_2	$12 \rightarrow 13$	266.82_8	266.42_0
$5 \rightarrow 6$	124.82_0	124.63_9	$13 \rightarrow 14$	286.56_4	286.13_6
$6 \rightarrow 7$	145.43_9	145.22_1	$14 \rightarrow 15$	306.12_7	305.66_9
$7 \rightarrow 8$	165.96_3	165.71_4			

* D. H. Martin, "Spectroscopic Techniques," North-Holland Publishing Company, Amsterdam, 1967.

TABLE 6r-8. PURE ROTATIONAL WATER-VAPOR ABSORPTION LINES*

Wave number, cm^{-1}	Intensity,† $grams/cm^2$	Assignment						Wave number, cm^{-1}	Intensity,† $grams/cm^2$	Assignment					
0.742	0.01	6	1	6	5	2	3	73.262	7,170	3	3	0	3	2	1
6.115	2.63	3	1	3	2	2	0	74.109	7,350	5	1	4	5	0	5
10.846	3.06	5	1	5	4	2	2	74.881	113	8	3	6	7	4	3
12.683	28.0	4	1	4	3	2	1	75.523	10,100	4	2	3	4	1	4
14.645	2.37	6	4	3	5	5	0	77.322	280	9	4	5	9	3	6
14.944	29.2	4	2	3	3	3	0	78.200	2,690	7	2	5	7	1	6
15.834	3.67	5	3	3	4	4	0	78.918	2,670	3	3	1	3	2	2
18.577	1,790	1	1	0	1	0	1	79.774	10,100	4	0	4	3	1	3
20.705	19.1	5	3	2	4	4	1	80.999	404	9	3	6	9	2	7
25.085	1,180	2	1	1	2	0	2	81.622	254	8	4	4	8	3	5
30.561	48.4	4	2	2	3	3	1	82.155	9,700	4	3	2	4	2	3
32.367	54.3	5	2	4	4	3	1	85.636	351	7	3	4	6	4	3
32.958	858	2	0	2	1	1	1	87.760	2,900	5	3	3	5	2	4
36.604	5,590	3	1	2	3	0	3	88.076	39,600	4	1	4	3	0	3
37.137	1,710	1	1	1	0	0	0	88.882	1,840	7	4	3	7	3	4
38.245	3.65	7	2	5	8	1	8	89.583	3,060	5	2	4	5	1	5
38.464	862	3	1	2	2	2	1	92.528	34,200	2	2	1	1	1	0
38.640	82.0	6	3	4	5	4	1	96.070	6,000	6	3	4	6	2	5
38.790	6,090	3	2	1	3	1	2	96.208	2,110	6	1	5	6	0	6
38.965	3.66	8		4	7	6	1	96.231	1,230	6	4	2	6	3	3
39.113	6.66	7	4	4	6	5	1	98.808	793	6	2	4	5	3	3
39.715	1.27	8	5	3	7	6	2	99.025	10,900	2	2	0	1	1	1
40.283	1,900	4	2	2	4	1	3	99.095	12,100	5	1	4	4	2	3
40.988	1,640	2	2	0	2	1	1	100.026	555	8	2	6	8	1	7
42.640	23.9	7	4	3	6	5	2	100.509	42,600	5	0	5	4	1	4
43.240	23.1	8	2	7	7	3	4	101.529	5,780	5	4	1	5	3	2
43.639	1.65	8	4	5	9	1	8	104.293	1,960	4	4	0	4	3	1
44.099	192	6	2	5	5	3	2	104.573	15,700	5	1	5	4	0	4
44.859	1.22	7	4	4	8	1	7	105.592	6,020	4	4	1	4	3	2
47.055	4,860	5	2	3	5	1	4	105.659	7,150	6	2	5	6	1	6
48.058	31	7	2	6	6	3	3	106.147	2,090	5	4	2	5	3	3
53.444	2,360	4	1	3	4	0	4	107.091	1,250	7	3	5	7	2	6
55.405	6,190	2	2	1	2	1	2	107.747	4,500	6	4	3	6	3	4
55.701	14,700	2	1	2	1	0	1	111.051	880	7	4	4	7	3	5
57.265	13,800	3	0	3	2	1	2	111.124	13,500	3	2	2	2	1	1
58.777	1,040	6	3	3	6	2	4	116.596	1,340	8	4	5	8	3	6
59.871	1,270	6	2	4	6	1	5	117.066	288	9	5	4	9	4	5
59.950	1,670	7	3	4	7	2	5	117.969	4,560	7	1	6	7	0	7
62.301	5,330	5	3	2	5	2	3	120.072	15,000	6	0	6	5	1	5
63.996	989	5	2	3	4	3	2	120.523	2,070	8	3	6	8	2	7
64.022	3,090	3	2	2	3	1	3	121.905	46,700	6	1	6	5	0	5
67.149	281	8	3	5	8	2	6	122.415	155	8	3	5		4	4
68.462	2,500	4	3	1	4	2	2	122.847	895	9	2	7	9	1	8
69.196	1,700	4	1	3	3	2	2	123.128	1,610	7	2	6	7	1	7
72.187	9,130	3	1	3	2	0	2	124.137	256	8	5	3	8	4	4

TABLE 6r-8. PURE ROTATIONAL WATER-VAPOR ABSORPTION LINES* (*Continued*)

Wave number, cm^{-1}	Intensity,† grams/cm	Assignment						Wave number, cm^{-1}	Intensity,† grams/cm^2	Assignment					
124.659	200	9	4	6	9	3	7	173.282	4,300	8	1	7	7	2	6
126.697	5,740	6	1	5	5	2	4	173.500	8,370	4	2	2	3	1	3
126.995	41,500	4	2	3	3	1	2	176.010	18,200	9	0	9	8	1	8
128.599	1,650	7	5	2	7	4	3	176.151	6,080	9	1	9	8	0	8
130.856	909	6	5	1	6	4	2	177.540	22,600	4	3	1	3	2	2
131.742	2,990	5	5	0	5	4	1	178.474	235	0	1	9	0	0	0
131.877	2,770	6	5	2	6	4	3	178.663	271	7	7	0	7	6	1
131.904	578	7	5	3	7	4	4	179.073	709	0	2	9	0	1	0
131.966	1.000	5	5	1	5	4	2	179.106	200	8	7	2	8	6	3
132.459	871	8	5	4	8	4	5	181.389	14,500	8	2	7	7	1	6
132.658	33,000	3	2	1	2	1	2	183.465	1,120	5	3	2	5	0	5
133.433	3.450	7	2	5	6	3	4	188.189	15,700	5	3	3	4	2	2
134.097	124	9	5	5	9	4	6	193.480	7,990	9	1	8		2	7
135.213	241	0	4	7	0	3	8	194.328	3,410	0	0	0	9	1	9
135.855	338	9	3	7	9	2	8	194.387	10,200	1	1	0	9	0	9
137.385	139	0	5	6	0	4	7	195.804	2,650	9	2	7	8	3	6
138.823	935	8	1	7	8	0	8	197.256	108	0	3	7	9	4	6
138.993	38,800	7	0	7	6	1	6	197.498	2,810	9	2	8	8	1	7
139.785	13,100	7	1	7	6	0	6	197.719	297	1	1	0	1	0	1
140.711	12,500	5	2	4	4	1	3	202.470	29,700	6	3	4	5	2	3
141.435	2,880	8	2	7	8	1	8	202.690	89,800	4	4	1	3	3	0
144.958	139	0	2	8	0	1	9	202.915	30,000	4	4	0	3	3	1
148.655	535	3	3	0	3	0	3	208.451	47,400	5	3	2	4	2	3
149.054	26,400	3	3	1	2	2	0	210.884	476	5	4	1	5	1	4
150.515	80,000	3	3	0	2	2	1	212.566	5,100	1	0	1	0	1	0
151.303	17,000	7	1	2	6	2	5	212.591	1,700	1	1	1	0	0	0
152.507	444	0	3	8	0	2	9	212.633	1,410	0	1	9	9	2	8
153.455	30,300	6	2	5	5	1	4	213.924	5,690	7	3	5	6	2	4
154.088	208	9	0	3	9	5	4	214.556	4,330	0	2	9	9	1	8
155.736	159	8	6	2	8	5	3	214.855	218	6	3	3	6	0	6
156.372	867	7	6	1	7	5	2	214.878	217	6	4	2	6	1	5
156.447	350	6	6	0	6	5	1	215.126	362	3	3	1	2	0	2
156.451	483	8	6	3	8	5	4	216.876	112	2	2	1	2	1	2
156.480	1,050	6	6	1	6	5	2	221.673	15,800	5	2	3	4	1	4
156.556	290	7	6	2	7	5	3	221.735	518	0	2	8	0	3	7
157.588	9,510	8	0	8	7	1	7	223.712	9,060	8	3	6	7	2	5
157.923	28,700	8	1	8	7	0	7	226.273	21,200	5	4	2	4	3	1
158.904	1,500	9	1	8	9	0	9	227.030	523	7	4	3	7	1	6
160.169	505	9	2	8	9	1	9	227.825	64,300	5	4	1	4	3	2
160.207	443	9	3	6	8	4	5	230.732	756	2	0	2	1	1	1
161.789	385	4	3	1	4	0	4	230.743	2,270	2	1	2	1	0	1
165.829	169	1	2	9	1	1	0	231.213	1,960	1	1	0	0	2	9
166.217	1,170	8	2	6	7	3	5	231.874	188	1	3	8	0	4	7
166.704	7,410	7	2	6	6	1	5	232.118	659	1	2	0	0	1	9
170.359	66,200	4	3	2	3	2	1	233.327	1,490	9	3	7	8	2	6

TABLE 6r-8. PURE ROTATIONAL WATER-VAPOR ABSORPTION LINES* (*Continued*)

Wave number, cm^{-1}	Intensity,† grams/cm^2	Assignment						Wave number, cm^{-1}	Intensity,† grams/cm^2	Assignment					
244.216	2,040	0	3	8	9	2	7	311.744	146	2	4	9	1	3	8
244.535	737	1	2	9	0	3	8	314.741	382	4	4	1	3	1	2
244.934	8,020	6	3	3	5	2	4	315.088	3,060	8	4	4	7	3	5
245.753	3,690	4	3	2	3	0	3	323.633	5,330	6	3	4	5	0	5
247.915	38,500	6	4	3	5	3	2	323.935	9,280	8	5	4	7	4	3
248.826	904	3	0	3	2	1	2	327.571	5,060	7	6	2	6	5	1
248.831	301	3	1	3	2	0	2	327.610	15,200	7	6	1	6	5	2
249.477	268	2	1	1	1	2	0	328.173	3,160	8	5	3	7	4	4
249.900	808	2	2	1	1	1	0	334.617	435	5	4	2	4	1	3
253.814	13,200	6	4	2	5	3	3	335.160	4,700	7	2	5	6	1	6
253.946	20,500	5	5	1	4	4	0	340.556	1,710	8	3	5	7	2	6
253.975	61,600	5	5	0	4	4	1	343.212	1,220	9	5	5	8	4	4
256.117	272	7	3	4	7	0	7	349.792	3,160	7	7	1	6	6	0
257.109	281	1	3	9	0	2	8	349.792	9,500	7	7	0	6	6	1
266.199	6,600	7	4	4	6	3	3	351.786	7,120	8	6	3	7	5	2
266.843	108	4	0	4	3	1	3	352.000	2,380	8	6	2	7	5	3
266.845	325	4	1	4	3	0	3	354.125	3,390	9	4	5	8	3	6
267.552	295	3	1	2	2	2	1	354.595	3,850	9	5	4	8	4	5
271.851	316	2	3	0	1	2	9	357.270	2,370	6	4	3	5	1	4
276.150	2,960	6	2	4		1	5	358.492	1,250	0	5	6	9	4	5
277.430	123	7	5	2	7	2	5	369.343	124	1	5	7	0	4	6
278.263	37,700	6	5	2	5	4	1	370.002	1,250	7	3	5	6	0	6
278.523	12,600	6	5	1	5	4	2	374.521	4,420	8	7	2	7	6	1
280.358	8,840	8	4	5	7	3	4	374.527	1,470	8	7	1	7	6	2
281.168	101	9	4	5	9	1	8	375.342	976	9	6	4	8	5	3
281.915	1,870	5	3	3	4	0	4	376.224	2,940	9	6	3	8	5	4
282.263	20,800	7	4	3		3	4	376.377	100	2	5	8	1	4	7
284.381	103	3	2	1	2	3	0	383.826	447	0	5	5	9	4	6
284.778	105	5	0	5	4	1	4	384.845	904	7	4	4	6	1	5
289.451	12,500	7	3	4	6	2	5	385.502	400	5	4	1	4	1	4
290.737	1,180	9	4	6	8	3	5	394.272	2,360	8	8	1	7	7	0
298.430	1,310	0	4	7	9	3	6	394.272	786	8	8	0	7	7	1
301.871	6,710	7	5	3	6	4	2	396.435	791	8	2	6	7	1	7
303.001	28,500	6	6	1	5	5	0	397.325	1,950	9	3	6	8	2	7
303.005	9,510	6	6	0	5	5	1	397.681	1,050	0	6	5	9	5	4
303.116	20,300	7	5	2	6	4	3	398.959	606	9	7	3	8	6	2
304.895	151	1	4	8	0	3	7	398.994	1,820	9	7	2	8	6	3
309.474	116	6	4	3	6	1	6								

* Only the following lines are included in the table:

$50 < \nu < 400$ cm^{-1}	and	$I > 100$
$1 < \nu < 50$ cm^{-1}	and	$I > 1$
$\nu < 1$ cm^{-1}	all	

Private communication from Clough, S. A. and W. S. Benedict.
† Intensity values are good at best to three significant figures.

6r-5. Far-infrared Polarizers. Polarizers for the far infrared have been made of stacks of dielectric plates at the Brewster angle, wire grids, and pyrolitic graphite. In addition, a Michelson interferometer acts as a polarizer when the radiant flux is incident on the beam splitter at the Brewster angle (cf. section on beam splitters).

Pile-of-plates polarizers have been discussed by Bird and Schurcliff [1], and a polarizer using polyethylene sheets has been reported by Mitsuishi et al [2]. The light is incident on the plates at the Brewster angle, and the polarizance of the device is

$$P = \frac{1 - \left(\frac{2n}{n^2+1}\right)^{4m}}{1 + \left(\frac{2n}{n^2+1}\right)^{4m}} \tag{6r-1}$$

where n is the refractive index and m the number of plates. (Polarizance is defined as the percent polarization of the output beam when the input is completely unpolarized.) For far-infrared polarizers two different plate thicknesses must be used to avoid interference effects which seriously reduce the polarizance at certain wavelengths. This polarizer is more easily built in the laboratory than the grating polarizer, but occupies more instrument space. Figure 6r-11 illustrates the polarizance of pile-of-plates polarizers using various combinations of polyethylene ($n = 1.5$) sheets. Equation (6r-1) gives $P = 88$ percent with 10 sheets and 97.5 percent with 15 sheets.

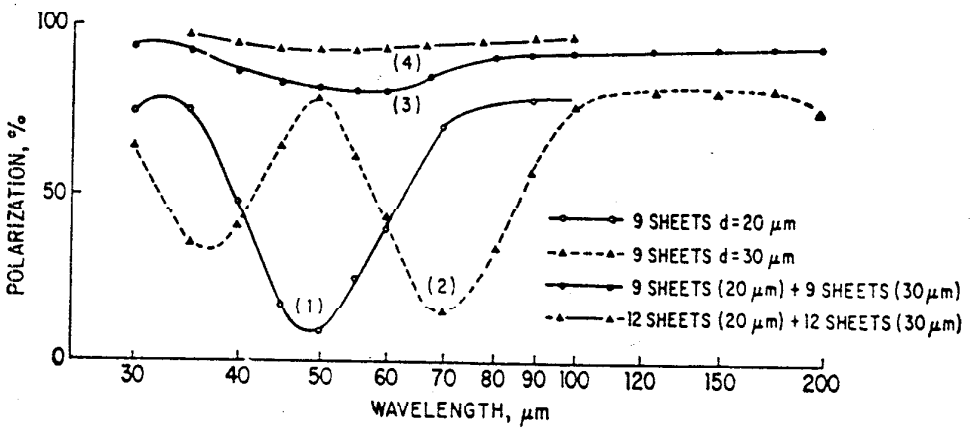

FIG. 6r-11. Degree of polarization with different numbers and thicknesses of polyethylene sheets.

The wire grid operates on the principle (discovered by Hertz) that radiation polarized parallel to the grids is reflected, while that polarized perpendicular is transmitted, for wavelengths larger than the grid constant. These polarizers have been made by evaporating metal at a large angle of incidence onto transmission gratings of the appropriate spacing so that one side of each groove is coated while the other remains transparent. The results obtained by Hass and O'Hara [3] are summarized in Tables 6r-9 and 6r-10, and the transmittance of their polarizers is shown in Fig. 6r-12.

TABLE 6r-9. DESCRIPTIONS OF POLARIZERS

Designation	Source of grating	Substrate and thickness	Conductor	Periodicity
DP1	Diffraction products	Polymethyl methacrylate, 0.051 mm	Aluminum (lightly coated)	2,160 grooves/mm* = 0.463 μm/groove
DP2	Diffraction products	Polymethyl methacrylate, 0.051 mm	Aluminum (heavily coated)	2,160 grooves/mm* = 0.463 μm/groove
NRL	Naval Research Lab.	Polyethylene, 0.152 mm	Aluminum (medium coat)	600 grooves/mm* = 1.69 μm/groove
BM	Buckbee Mears	Mylar sheet, 0.038 mm	Gold strips 0.01 mm wide	39.3 lines/mm = 25.4 μm/line

* The blaze angle is about 20°.

TABLE 6r-10. TRANSMITTANCE AND DEGREE OF POLARIZATION

Wave number, cm^{-1}	Degree of polarization P, %				Transmittance T_1			
	DP1	DP2	NRL	BM	DP1	DP2	NRL	BM
2.5	99.0	....	....	>99.5	0.985	....	....	>0.995
49.5	97.8	....	96.4	98.4	0.86	....	0.87	0.81
83	98.8	....	97.9	98.4	0.86	....	0.88	0.86
160	98.9	99.0	98.0	89.0	0.86	0.80	0.83	0.67
300	98.1	....	96.6	.....	0.65	....	0.84	
600	98.2	....	96.0	.....	0.94	....	0.81	
1,025	96.3	99.4	89.0	.....	0.86	0.53	0.57	
2,000	88.0	99.5	63.0	.....	0.90	0.65	0.43	
3,500	71.0	98.4	33.0	.....	0.90	0.54	0.35	
5,710	....	95.0	....	.....	....	0.39		
10,000	....	84.1	....	.....	.....	0.27		

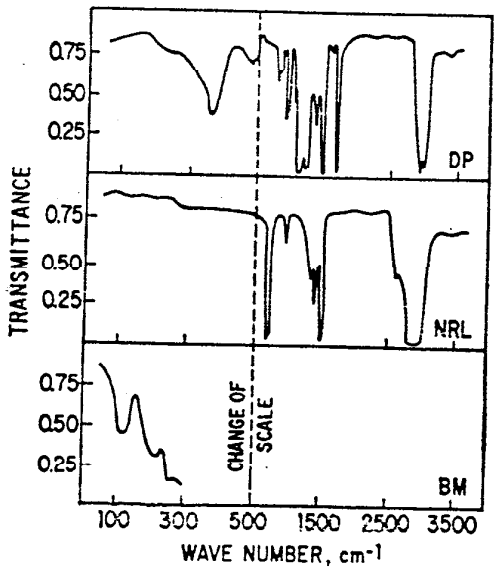

FIG. 6r-12. Transmittance of gratings. The DP polymethyl methacrylate grating and the NRL polyethylene grating were unaluminized and measured in unpolarized radiation. The BM metal-strip grating was measured in the high-transmission direction in polarized radiation.

TABLE 6r-11. TRANSMITTANCE OF PYROGRAPHITE POLARIZER PGP1 FOR RADIATION WITH ELECTRIC FIELD IN THE *c* DIRECTION

Wave number, cm^{-1}	$T_1 \pm 2\%$
17.1	0.519
22.7	0.504
33.3	0.512
42.0	0.487
51.0	0.495
58.8	0.519
66.2	0.520
71.0	0.505
77.0	0.507
81.5	0.494

TABLE 6r-12. PERCENTAGE POLARIZATION OF PYROGRAPHITE POLARIZER PGP1

Wave number, cm^{-1}	$T_2 \times 10^3$*	Percentage polarization
16.7	1.7	99.65 ± 0.35
21.7	4.5	99.11 ± 0.21
28.6	2.4	99.53 ± 0.06
500	7.5	98.03
666.7	10.7	97.45
1,000	11.4	96.20
2,000	7.7	93.58

* T_2 is the transmittance for the unwanted direction of polarization.

A thin foil of pyrolitic graphite, which has a layered crystal structure, acts as a polarizer [4] in both the far and the near infrared. The transmittance for the desired polarization is rather low (about 50 percent), but the polarizance is above 99 percent. The results obtained by Rupprecht et al. [4] are summarized in Tables 6r-11 and 6r-12.

References for Sec. 6r-5

1. Bird, G. R., and W. A. Schurcl ff: *J. Opt. Soc. Am.* **49**, 235 (1959).
2. Mitsuishi, A., Y. Yamada, S. Fujita, and H. Yoshinaga: *J. Opt. Soc. Am.* **50**, 433 (1960).
3. Hass, M., and M. O'Hara: *Appl. Opt.* **4**, 1027 (1965).
4. Rupprecht, G., D. M. Ginsberg, and J. D. Leslie: *J. Opt. Soc. Am.* **52**, 665 (1962).

6r-6. Optical Constants of Far-infrared Materials. Precise values of refractive index and reasonably good values of absorption coefficient have been determined for far-infrared materials by two techniques. Both are basically interferometric: one is the use of a Michelson Fourier spectrometer with the sample in one arm [1,2], referred to as an "asymmetric Michelson"; the other is the analysis of the channel-spectrum fringes (fringes of equal chromatic order) resulting from interference between the multiple beams produced by internal reflections in a plane-parallel sample of material [3]. In the asymmetric Michelson method, the sample is placed in one arm, and an interferogram is taken; the amplitude of the resulting spectrum gives the absorption coefficient while the phase gives the refractive index. The analysis of the channel spectra is based on the fact that the fringe position depends on the index only, whereas the amplitude depends on both index and absorption coefficient. The channel-spectrum fringes are revealed by spectra, which may be taken with either a conventional or a Fourier spectrometer.

In spite of the fact that the absorption coefficient can in theory be derived by the above methods, in most of the data given below it is derived from analysis of a low-

resolution transmission spectrum, using the refractive index found in the interferometric method. This is so because discrepancies between absorption coefficients calculated from the asymmetric Michelson or channel spectrum and those calculated from the transmission measurements are always resolved in favor of the latter.

The tables and graphs below list the optical constants for the following materials:

Crystal quartz	Mylar (polyethylene terephthalate)
Sapphire	Irtran VI (hot-pressed CdTe)
Germanium	Teflon (polytetrafluoroethylene)
Silicon	CdTe (crystalline)
Fused quartz	GaAs (crystalline)

The quantites given are index and absorption coefficient α which is related to k, the imaginary part of the complex refractive index, by

$$\alpha = 4\pi k\sigma$$

where σ = wave number of the radiation. Units of σ and α are cm^{-1} in all cases. Except where noted, measurements were made at room temperature.

The optical constants of Mylar are labeled with subscripts 1 and 2. *If* Mylar is uniaxial, 1 denotes the ordinary optical constants, 2 the extraordinary. Mylar is probably biaxial, but it is difficult to determine this for the far infrared. The samples were aligned by using a polarizing microscope.

TABLE 6r-13. OPTICAL CONSTANTS OF CRYSTAL QUARTZ FROM 20 TO 200 cm^{-1}*

Wave number, σ, cm^{-1}	Refractive indices†			Absorption coefficients,‡ cm^{-1}	
	n_0	n_e	$n_e - n_0$	α_0	α_e
20.2	2.1073	2.1541	0.0468		
25.2	2.1076	2.1561	0.0485		
30.2	2.1076	2.1560	0.0484	0.10	0.10
35.3	2.1083	2.1564	0.0481		
40.3	2.1093	2.1573	0.0480		
45.4	2.1105	2.1580	0.0475	0.15	0.12
50.4	2.1114	2.1590	0.0476		
55.4	2.1124	2.1602	0.0478		
60.5	2.1134	2.1615	0.0481	0.32	0.21
65.5	2.1147	2.1629	0.0482		
70.6	2.1159	2.1644	0.0485		
75.6	2.1175	2.1662	0.0487	0.47	0.37
80.6	2.1190	2.1679	0.0489		
85.7	2.1209	2.1699	0.0490		
90.7	2.1228	2.1718	0.0490	0.61	0.56
95.8	2.1248	2.1739	0.0491		
100.8	2.1269	2.1762	0.0493		
105.8	2.1291	2.1787	0.0496	0.90	0.83
110.9	2.1316	2.1815	0.0499		
115.9	2.1343	2.1842	0.0499		
120.9	2.1376	2.1872	0.0496	1.2	1.1
122.0	2.1383	(2.1877) §	0.0494	1.3	
123.0	2.1393	(2.1882)	0.0489	1.3	
124.0	2.1400	(2.1888)	0.0488	1.9	
125.0	2.1413	(2.1895)	0.0482	2.5	
126.0	2.1421	2.1902	0.0481	4.3	
127.0	2.1426	(2.1909)	0.0483	6.0	
128.0	2.1419	(2.1916)	0.0497	8.5	
129.0	2.1408	(2.1923)	0.0515	8.0	
130.0	2.1403	(2.1930)	0.0527	7.1	
131.0	2.1406	2.1937	0.0531	5.3	
132.0	2.1413	(2.1944)	0.0531	4.7	
133.0	2.1419	(2.1950)	0.0531	3.8	
134.0	2.1428	(2.1957)	0.0529	3.6	
135.0	2.1434	(2.1964)	0.0530	3.1	
136.1	2.1441	2.1971	0.0530	2.8	1.3
141.1	2.1478	2.2009	0.0531		
146.1	2.1515	2.2049	0.0534		
151.2	2.1553	2.2089	0.0536	2.8	1.0
156.2	2.1592	2.2131	0.0539		
161.3	2.1635	2.2177	0.0542		
166.3	2.1678	2.2222	0.0544	3.3	2.4
171.3	2.1725	2.2273	0.0548		
176.4	2.1773	2.2325	0.0552		
181.4	2.1826	2.2381	0.0555	4.1	3.2
186.5	2.1882	2.2440	0.0558		
191.5	2.1941	2.2502	0.0561		
196.5	2.2005				
201.6	2.2072				

* E. E. Russell and E. E. Bell, *J. Opt. Soc. Am.* **57**, 341 (1967).

† The total, estimated probable error in the measured values of the refractive indices is ±0.001 except at wave numbers less than 25 cm^{-1} and greater than 175 cm^{-1}, where the error can be somewhat greater.

‡ The estimated probable error in the measured absorption coefficients is approximately ±100% for $\alpha < 0.2$; ±50% for $0.2 < \alpha < 0.4$; ±20% for $0.4 < \alpha < 0.8$; and ±10% for $\alpha > 0.8$.

§ The bracketed values of the extraordinary-ray refractive indices were interpolated from the neighboring values.

TABLE 6r-14. OPTICAL CONSTANTS OF SAPPHIRE FROM 20 TO 175 CM^{-1}*

Wave number, σ, cm^{-1}	Refractive indices†			Absorption coefficients,‡ cm^{-1}	
	n_o	n_e	$n_e - n_o$	α_o	α_e
20.2	3.0688	3.4111	0.3423		
25.2	3.0698	3.4129	0.3436		
30.2	3.0704	3.4134	0.3430	0.4	0.5
35.3	3.0720	3.4163	0.3443		
40.3	3.0740	3.4187	0.3447		
45.4	3.0752	3.4232	0.3480	1.7	2.2
50.4	3.0770	3.4260	0.3490		
55.4	3.0795	3.4294	0.3499		
60.5	3.0822	3.4334	0.3512	3.6	4.0
65.5	3.0843	3.4391	0.3548		
70.6	3.0870	3.4444	0.3574		
75.6	3.0906	3.4510	0.3604	4.9	7.6
80.6	3.0941	3.4569	0.3628		
85.7	3.0982	3.4625	0.3643		
90.7	3.1019	3.4689	0.3670	7.2	12.7
95.8	3.1060	3.4766	0.3706		
100.8	3.1103	3.4836	0.3733		
105.8	3.1147	3.4908	0.3761	9.9	17.8
110.9	3.1198	3.4993	0.3795		
115.9	3.1249	3.5081	0.3832		
120.9	3.1304	3.5185	0.3881	12.9	24.0
126.0	3.1357	3.5279	0.3922		
131.0	3.1422	3.5375	0.3953		
136.1	3.1485	3.5508	0.4023	15.7	29.6
141.1	3.1549	3.5612	0.4063		
146.1	3.1623	3.5746	0.4123		
151.2	3.1696	3.5856	0.4160	19.7	35.9
156.2	3.1765	3.6042	0.4277		
161.3	3.1854				
166.3	3.1921			26.2	
171.3	3.2018				
176.4	3.2113				

* E. E. Russell and E. E. Bell, *J. Opt. Soc. Am.* **57**, 543 (1967).

† The total estimated probable error of the measured values of the refractive indices is ±0.002 except at wave numbers less than 25 cm^{-1} and greater than 150 cm^{-1} where the error may be somewhat greater.

‡ The estimated probable error of the measured absorption coefficients is approximately 50% for $\alpha < 1.0$ cm^{-1}; ±20% for 1.0 $cm^{-1} < \alpha < 20$ cm^{-1}; ±30% for $\alpha > 20$ cm^{-1}.

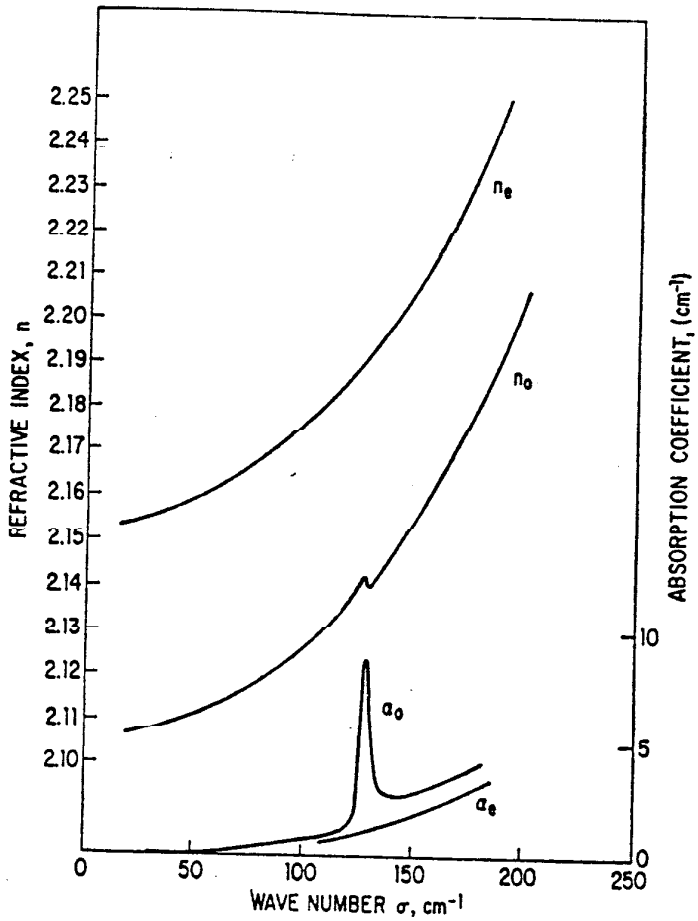

FIG. 6r-13*a*. Optical constants of crystal quartz from 20 to 200 cm^{-1}. [*E. E. Russell and E. E. Bell, J. Opt. Soc. Am.* **57**, 341 (1967).]

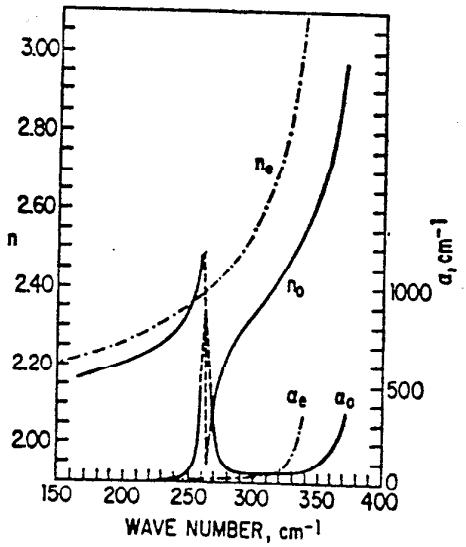

FIG. 6r-13*b*. Optical constants of crystal quartz from 150 to 370 cm^{-1}. [*E. E. Russell and E. E. Bell, J. Opt. Soc. Am.* **57**, 341 (1967).]

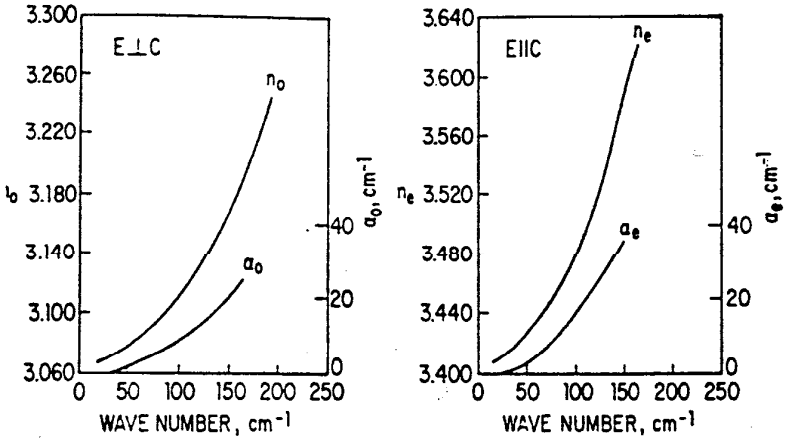

FIG. 6r-14. Optical constants of sapphire from 20 to 175 cm^{-1}: (*a*) ordinary ray and (*b*) extraordinary ray. [*E. E. Russell and E. E. Bell, J. Opt. Soc. Am.* **57**, 543 (1967).]

TABLE 6r-15. OPTICAL CONSTANTS OF GERMANIUM FROM 10 TO 140 CM^{-1}*

Wave number, cm^{-1}	Refractive index n	Wave number, cm^{-1}	Absorption coefficient, cm^{-1}	Wave number, cm^{-1}	Refractive index n	Wave number, cm^{-1}	Absorption coefficient, cm^{-1}
17.5	4.0041	10	1.05	92.5	4.00606	85	1.76
22.5	4.00452	15	1.02	97.5	4.00611	90	2.04
27.5	4.00480	20	1.14	102.5	4.00571	95	2.43
32.5	4.00509	25	1.08	107.5	4.00572	100	3.08
37.5	4.00535	30	1.05	112.5	4.00553	105	3.03
42.5	4.00540	35	0.99	117.5	4.00538	110	2.81
47.5	4.00567	40	0.84	122.5	4.00519	115	2.70
52.5	4.00570	45	0.73	127.5	4.0061	120	2.63
57.5	4.00590	50	0.73	132.5	4.0056	125	2.45
62.5	4.00610	55	0.81	137.5	4.0058	130	2.0
67.5	4.00627	60	0.87	142.5	4.0066	135	1.9
72.5	4.00631	65	1.00			140	1.9
77.5	4.00616	70	1.22				
82.5	4.00608	75	1.64				
87.5	4.00619	80	1.59				

* C. M. Randall and R. D. Rawcliffe, *Appl. Opt.* **6**, 1889 (1967).

TABLE 6r-16. OPTICAL CONSTANTS OF SILICON FROM 10 TO 140 CM^{-1}*

Wave number, cm^{-1}	Refractive index n	Wave number, cm^{-1}	Absorption coefficient, cm^{-1}	Wave number, cm^{-1}	Refractive index n	Wave number, cm^{-1}	Absorption coefficient, cm^{-1}
22.5	3.4172	10	0.54	87.5	3.41828	75	0.32
27.5	3.4167	15	0.52	92.5	3.41832	80	0.33
32.5	3.41753	20	0.54				
37.5	3.41756	25	0.56	97.5	3.41848	85	0.28
42.5	3.41779	30	0.58	102.5	3.41858	90	0.34
				107.5	3.41860	95	0.43
47.5	3.41790	35	0.60	112.5	3.41866	100	0.44
52.5	3.41791	40	0.48	117.5	3.41852	105	0.44
57.5	3.41796	45	0.43				
62.5	3.41807	50	0.44	122.5	3.41860	110	0.54
67.5	3.41818	55	0.46	127.5	3.41873		
				132.5	3.41873		
72.5	3.41824	60	0.34	137.5	3.4184		
77.5	3.41825	65	0.32	142.5	3.4188		
82.5	3.41824	70	0.33				

* C. M. Randall and R. D. Rawcliffe, *Appl. Opt.* **6**, 1889 (1967).

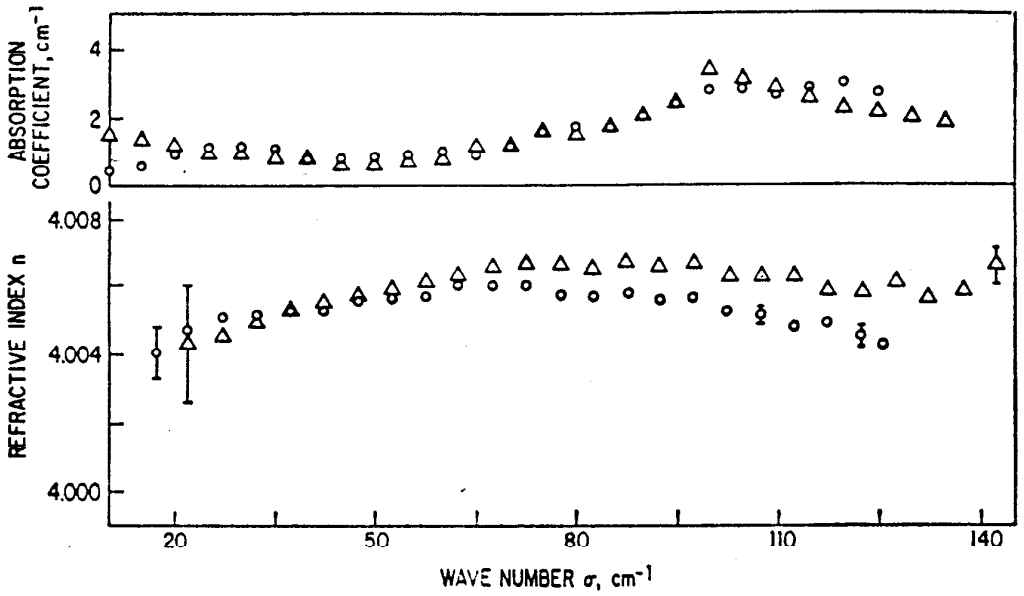

FIG. 6r-15. Optical constants of germanium from 10 to 140 cm^{-1}. Circles: 6-mm sample, triangles: 2-mm sample. [*C. M. Randall and R. D. Rawcliffe, Appl. Opt.* **7**, 213 (1968).]

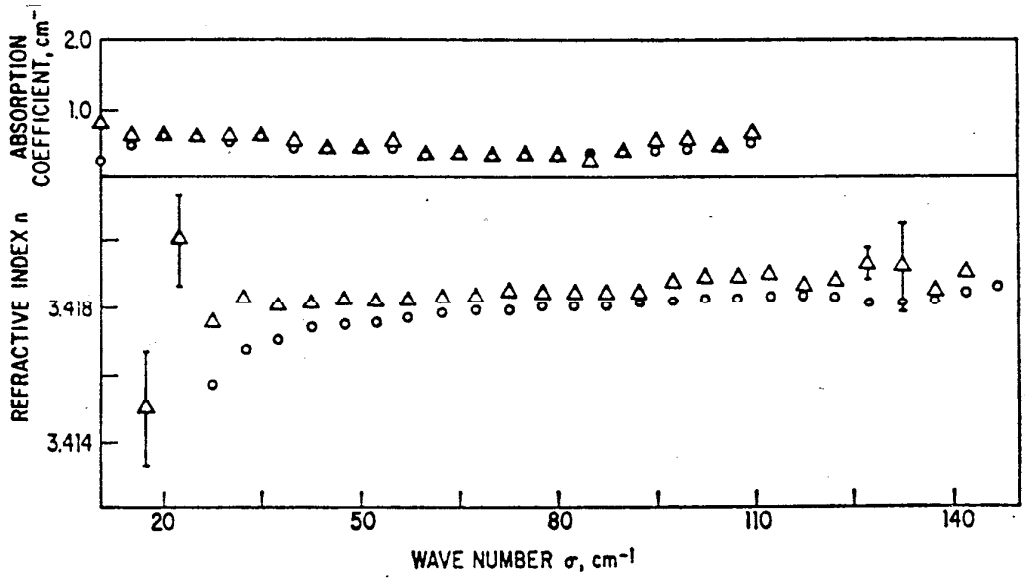

FIG. 6r-16. Optical constants of silicon from 10 to 140 cm^{-1}. Circles: 6-mm sample, triangles: 2-mm sample. [*C. M. Randall and R. D. Rawcliffe, Appl. Opt.* **7**, 213 (1968).]

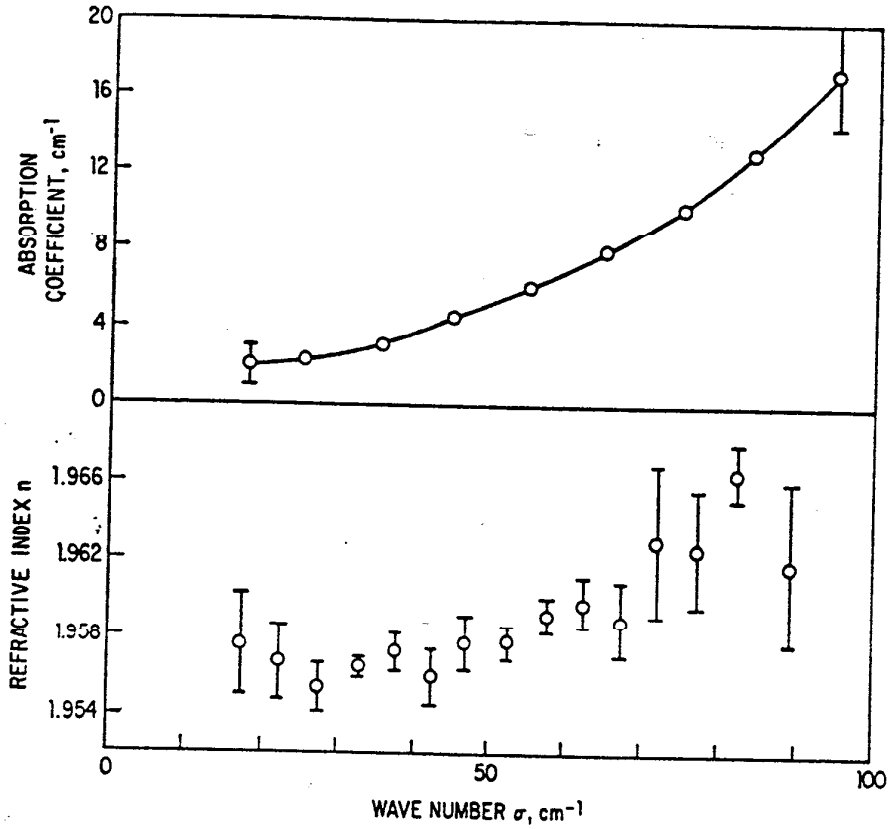

FIG. 6r-17. Optical constants of fused quartz from 15 to 95 cm^{-1}. [*C. M. Randall and R. D. Rawcliffe, Appl. Opt.* 7, 213 (1968).]

TABLE 6r-17. OPTICAL CONSTANTS OF FUSED QUARTZ FROM 15 TO 95 CM^{-1}*

Wave number, cm^{-1}	Refractive index n	Wave number, cm^{-1}	Absorption coefficient, cm^{-1}
17.32	1.9576	15	2.0
22.11	1.9567	25	2.3
27.48	1.9554	35	3.1
32.86	1.9565	45	4.6
37.63	1.9573	55	6.2
42.43	1.9560	65	8.0
46.72	1.9576	75	10.2
52.54	1.9576	85	13.0
57.89	1.9592	95	17.2
62.65	1.9598		
67.49	1.9589		
72.08	1.9630		
77.42	1.9626		
82.66	1.9665		
89.32	1.9618		

C. M. Randall and R. D. Rawcliffe, *Appl. Opt.* 6, 1889 (1967).

TABLE 6r-18. OPTICAL CONSTANTS OF MYLAR (POLYETHYLENE TEREPHTHALATE) FROM 40 TO 350 cm^{-1}*

σ	n_1	σ	n_2	σ	n_1	σ	n_2
55.29	1.7171	54.16	1.7525	209.84	1.6907	204.98	1.7305
61.17	1.7153	59.74	1.7561	215.57	1.6922	210.52	1.7324
67.06	1.7137	65.31	1.7593	221.37	1.6930	216.05	1.7343
72.94	1.7127	70.89	1.7618	227.34	1.6925	221.60	1.7360
78.84	1.7111	76.53	1.7624	233.61	1.6898	227.21	1.7371
84.85	1.7078	82.31	1.7602	239.98	1.6867	232.91	1.7375
91.01	1.7020	88.27	1.7546	246.07	1.6855	238.76	1.7368
97.25	1.6956	94.33	1.7478	251.92	1.6860	244.61	1.7361
103.33	1.6925	100.24	1.7443	257.69	1.6871	250.37	1.7361
109.23	1.6926	105.97	1.7444	263.45	1.6881	256.00	1.7369
115.01	1.6945	111.57	1.7464	269.26	1.6888	261.54	1.7383
120.76	1.6965	117.10	1.7492	275.18	1.6888	267.04	1.7399
126.59	1.6973	122.61	1.7521	281.24	1.6880	272.55	1.7414
132.63	1.6954	128.15	1.7543	287.25	1.6874	278.14	1.7423
139.05	1.6891	133.87	1.7540	293.03	1.6882	283.85	1.7425
145.45	1.6834	141.88	1.7555	298.58	1.6903	289.02	1.7423
151.49	1.6824	148.52	1.7158	303.95	1.6933	295.31	1.7425
157.31	1.6837	154.18	1.7176	309.20	1.6968	300.83	1.7437
163.04	1.6857	159.68	1.7209	314.34	1.7008	306.26	1.7455
168.77	1.6877	165.20	1.7239	319.42	1.7050	311.64	1.7474
174.58	1.6887	170.73	1.7265	324.48	1.7093	317.01	1.7493
180.50	1.6887	176.36	1.7281	329.52	1.7134	322.40	1.7510
186.51	1.6879	182.08	1.7287	334.57	1.7174	327.82	1.7525
192.49	1.6874	187.87	1.7286	339.62	1.7212	333.43	1.7530
198.36	1.6878	193.66	1.7285	344.63	1.7252	339.20	1.7526
204.13	1.6891	199.37	1.7291				

σ	α_1	α_2	σ	α_1	α_2
50.0	12.9	12.7	175.0	55.2	61.1
55.0	21.0	17.7	180.0	60.2	64.8
60.0	27.7	20.9	185.0	62.8	67.7
65.0	31.9	25.0	190.0	63.6	68.8
70.0	35.7	26.9	195.0	63.2	68.2
75.0	40.2	32.9	200.0	62.4	66.4
80.0	45.4	39.9	205.0	62.7	64.7
85.0	51.2	46.0	210.0	64.6	64.1
90.0	55.1	50.0	215.0	68.9	65.6
95.0	55.2	49.9	220.0	75.3	68.3
100.0	52.5	45.4	225.0	83.0	72.3
105.0	48.7	42.4	230.0	90.5	77.4
110.0	45.8	41.6	235.0	95.8	82.0
115.0	45.0	43.4	240.0	95.2	86.7
120.0	46.8	47.7	245.0	92.0	88.5
122.5	48.6	50.8	250.0	91.3	87.2
125.0	51.4	55.4	255.0	92.3	88.4
127.5	53.1	63.6	260.0	95.4	90.4
130.0	57.5	68.2	265.0	100.2	93.7
132.0	61.3	76.5	270.0	106.4	98.9
134.0	61.9	80.7	275.0	114.3	104.6
136.0	64.7	88.4	280.0	120.2	110.5
138.0	66.4	109.2	285.0	122.0	115.8
140.0	66.8	123.0	290.0	121.7	118.1
142.0	65.0	117.8	295.0	121.1	114.4
144.0	61.8	104.5	300.0	121.7	108.8
146.0	62.3	86.8	305.0	123.8	111.0
148.0	58.3	79.7	310.0	126.7	111.8
150.0	54.8	74.7	315.0	130.0	114.1
152.5	53.9	67.0	320.0	133.0	118.8
155.0	51.0	63.3	325.0	135.4	124.0
157.5	49.5	60.0	330.0	137.7	132.4
160.0	49.0	59.4	335.0	140.5	140.7
165.0	49.3	57.1	340.0	144.3	151.6
170.0	51.7	57.8			

* Unpublished work of the subsection authors.

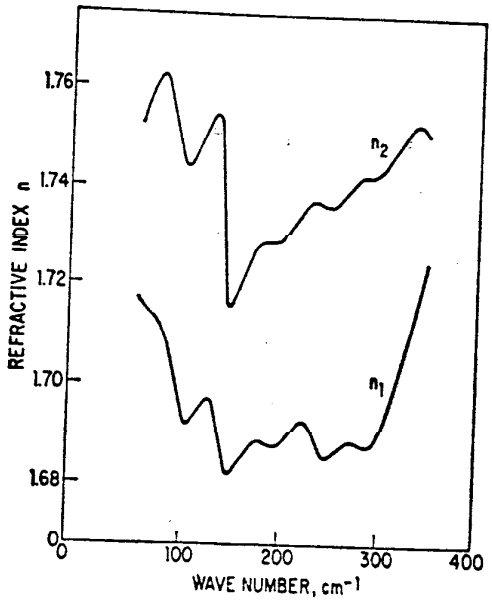

(*a*) Refractive indices.

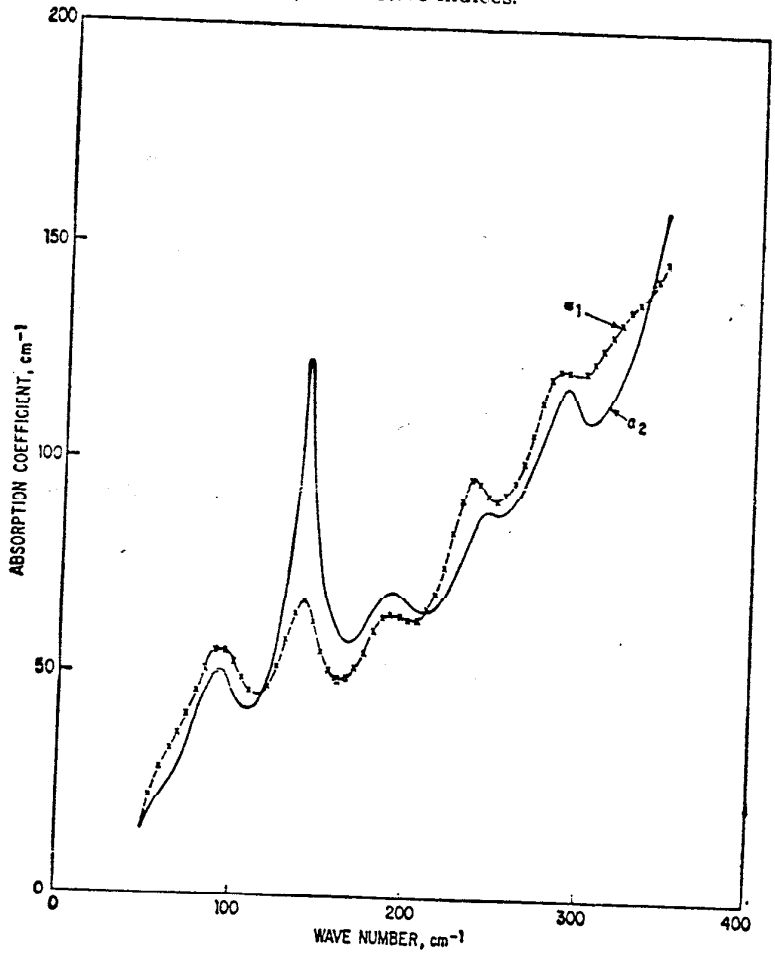

(*b*) Absorption coefficients.

FIG. 6r-18. Optical constants of Mylar from 40 to 350 cm^{-1}. [*E. V. Loewenstein and D. R. Smith, Appl. Opt.* **10**, 577 (1971).]

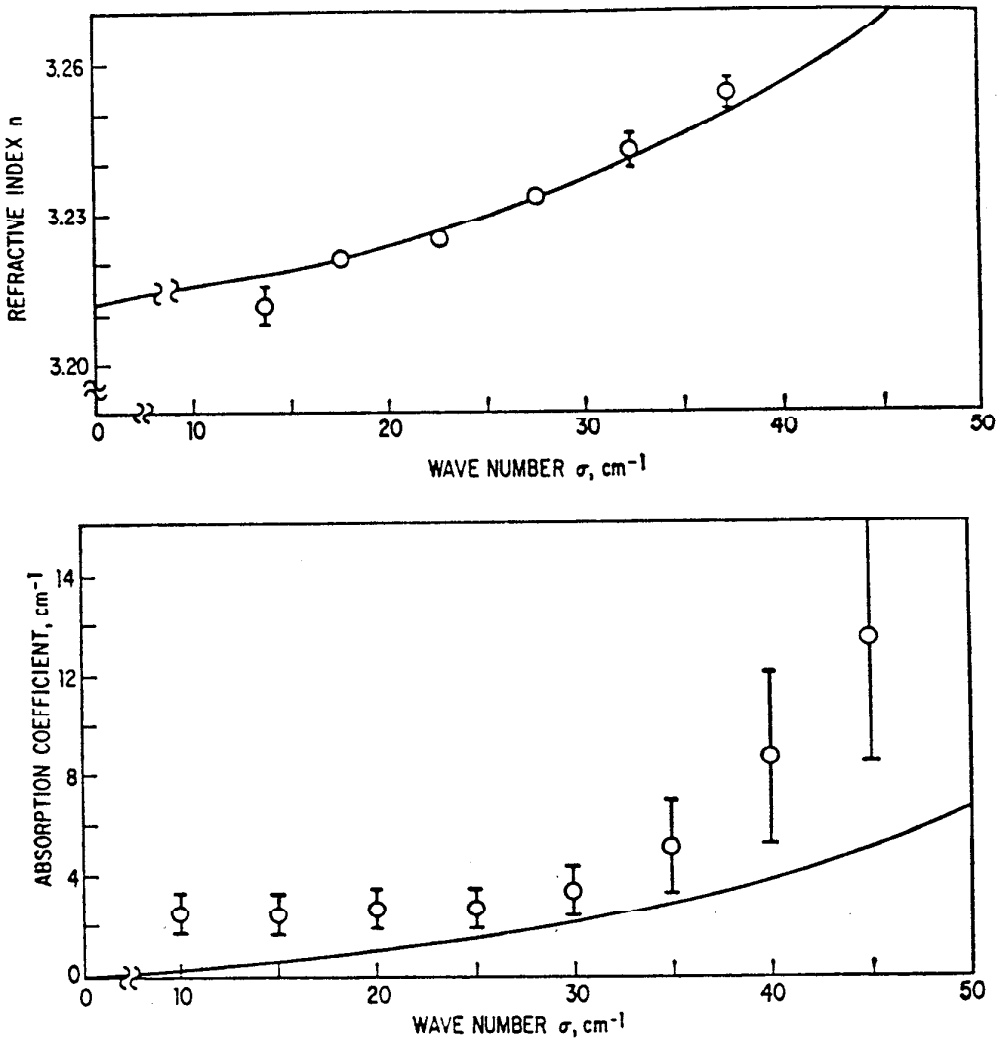

FIG. 6r-19. Optical constants of Irtran VI (hot pressed CdTe) from 10 to 45 cm^{-1}. The solid line on the absorption coefficient graph was calculated using a Lorentz oscillator model based on the index measurements. [*C. M. Randall and R. D. Rawcliffe, Appl. Opt.* **7**, 213 (1968).]

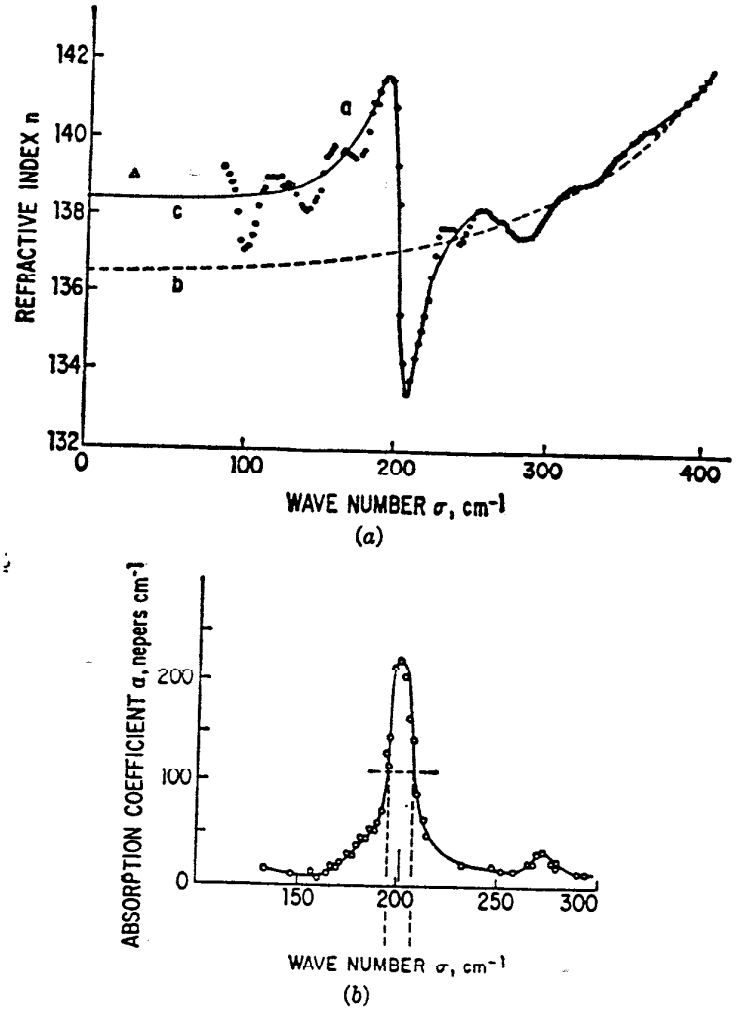

FIG. 6r-20. Optical constants of Teflon (polytetrafluoroethylene) from 100 to 350 cm^{-1}. (*a*) Refractive index—circles are the experimental points including channel-spectrum fringes. Solid line is drawn through the average value of the experimental points. Dashed line represents the calculated contribution to the index from absorption at higher wave numbers. (*b*) Absorption coefficient. [*J. E. Chamberlain and H. A. Gebbie, Appl. Opt.* **5**, 393 (1966).]

TABLE 6r-19. OPTICAL CONSTANTS OF IRTRAN VI (HOT-PRESSED CdTe) FROM 10 TO 45 cm^{-1}*

Wave number, cm^{-1}	Refractive index n	Wave number, cm^{-1}	Absorption coefficient, cm^{-1}
13.73	3.212	10	2.5
17.68	3.221	15	2.4
22.63	3.225	20	2.7
27.53	3.233	25	2.7
32.40	3.243	30	3.4
37.23	3.254	35	5.1
		40	8.7
		45	13.4

* C. M. Randall and R. D. Rawcliffe, *Appl. Opt.* **7**, 213 (1968).

TABLE 6r-20. OPTICAL CONSTANTS OF CdTe FROM 33 TO 833 cm^{-1}, AT 300 K AND FROM 33 TO 400 cm^{-1} AT 8 K*

Temperature, 300 K			Temperature, 8 K		
Wave number, cm^{-1}	Index n	Absorption coefficient	Wave number, cm^{-1}	Index n	Absorption coefficient
833	2.57	0.3	400	2.52	0.5
769	2.57	0.3	370	2.51	0.6
667	2.56	0.3	345	2.49	0.9
500	2.54	0.4	323	2.47	1.8
454	2.53	0.4	313	2.46	6.4
417	2.52	0.5	300	2.45	17.0
385	2.51	0.7	286	2.43	5.2
357	2.49	0.9	278	2.42	3.6
333	2.47	2.5	270	2.40	5.7
323	2.46	4.6	263	2.39	8.0
313	2.45	10.0	256	2.37	8.5
286	2.42	Very large	244	2.33	4.1
250	2.34	Very large	233	2.29	3.4
222	2.22	Very large	222	2.24	3.0
200	2.03	Very large	213	2.17	5.3
100	3.49	Very large	200	2.04	17.0
90	3.37	Very large	192	1.92	Very large
77	3.25	Very large	132	4.43	Very large
67	3.19	Very large	128	4.15	12.0
59	3.16	Very large	125	3.96	7.0
53	3.14	14.0	119	3.71	3.4
50	3.13	10.0	113	3.56	2.4
45	3.12	6.6	108	3.44	2.3
40	3.11	4.2	100	3.33	2.8
37	3.10	3.5	89	3.23	3.7
36	3.10	3.3	83	3.18	3.2
33	3.09	3.0	80	3.16	2.9
			77	3.15	2.9
			74	3.13	2.8
			71	3.12	2.0
			67	3.10	0.7
			63	3.09	0.3
			59	3.08	0.1
			56	3.07	<0.1
			53	3.06	<0.1
			50	3.05	<0.1
			40	3.03	<0.1
			33	3.02	<0.1

* C. J. Johnson, G. H. Sherman, and R. Weil, *Appl. Opt.* **8**, 1667 (1969).

TABLE 6r-21. OPTICAL CONSTANTS OF GaAs FROM 33 TO 833 cm^{-1} AT 300 K AND FROM 33 TO 400 cm^{-1} AT 8 K

Temperature, 300 K						Temperature, 8 K		
Wave number, cm^{-1}	Index n	Absorption coefficient	Wave number, cm^{-1}	Index n	Absorption coefficient	Wave number, cm^{-1}	Index n	Absorption coefficient
833	3.27	0.1	333	2.71	Very large	426	3.12	1.4
813	3.27	0.2	238	4.44	Very large	400	3.07	1.9
769	3.26	0.3	233	4.30	Very large	370	2.98	4.0
714	3.25	0.2	222	4.11	Very large	357	2.92	8.2
667	3.25	0.2	213	4.00	Very large	345	2.83	21.0
625	3.24	0.5	204	3.92	Very large	333	2.72	Very large
588	3.23	0.7	196	3.87	Very large	263	5.86	Very large
556	3.21	4.3	172	3.76	17.0	256	5.01	18.0
526	3.20	21.0	167	3.74	14.0	250	4.62	16.0
500	3.18	Very large	143	3.68	6.7	222	3.99	4.5
476	3.16	Very large	125	3.65	4.9	200	3.82	2.9
454	3.14	Very large	111	3.63	4.1	167	3.69	1.4
435	3.12	15.0	100	3.62	3.6	143	3.64	0.5
426	3.10	12.0	83	3.61	2.8	125	3.61	0.2
413	3.08	13.0	74	3.60	2.4	111	3.60	0.1
394	3.04	9.0	67	3.60	1.8	100	3.59	<0.1
385	3.01	13.0	59	3.59	1.2	67	3.57	<0.1
370	2.96	21.0	50	3.59	0.5	33	3.55	<0.1
357	2.90	Very large	40	3.58	0.1			
345	2.82	Very large	33	3.58	<0.1			

References for Sec. 6r-6

1. Bell, E. E.: *Infrared Phys.* **6**, 57 (1966).
2. Chamberlain, J. E., J. E. Gibbs, and H. A. Gebbie: *Nature* **198**, 874 (1963).
3. Randall, C. M., and R. D. Rawcliffe: *Appl. Opt.* **6**, 1889 (1967).
4. Russell, E. E., and E. E. Bell: *J. Opt. Soc. Am.* **57**, 341 (1967).
5. Russell, E. E., and E. E. Bell: *J. Opt. Soc. Am.* **57**, 543 (1967).
6. Randall, C. M., and R. D. Rawcliffe: *Appl. Opt.* **7**, 213 (1968).
7. Unpublished work of the subsection authors.
8. Chamberlain, J. E., and H. A. Gebbie: *Appl. Opt.* **5**, 393 (1966).
9. Johnson, C. J., G. H. Sherman, and R. Weil: *Appl. Opt.* **8**, 1667 (1969).

6r-7. Beam Splitters for the Far Infrared. Michelson interferometers for the far infrared may employ as beam splitters either a metal mesh or an uncoated Mylar (polyethylene terephthalate) film. For maximum efficiency, any beam splitter should have $R \approx T \approx \frac{1}{2}$, where R and T are the intensity reflection and transmission coefficients.

For the dielectric film beam splitter the efficiency may be calculated directly in terms of the optical constants, since R and T are given by the Fresnel coefficients. The efficiency is [1]

$$\varepsilon = \frac{8RT^2(1 - \cos(4\pi n\sigma d \cos\theta'))}{[1 + R^2 - 2R\cos(4\pi n\sigma d \cos\theta')]^2}$$

where σ = wave number of the radiation
n = refractive index (at the wave number σ)
d = beam splitter thickness
θ' = angle between a ray and the surface normal *inside* the beam splitter film

Since R and T depend upon polarization, the beam splitter will affect the state of polarization of the emergent radiation. When the radiation is incident upon the

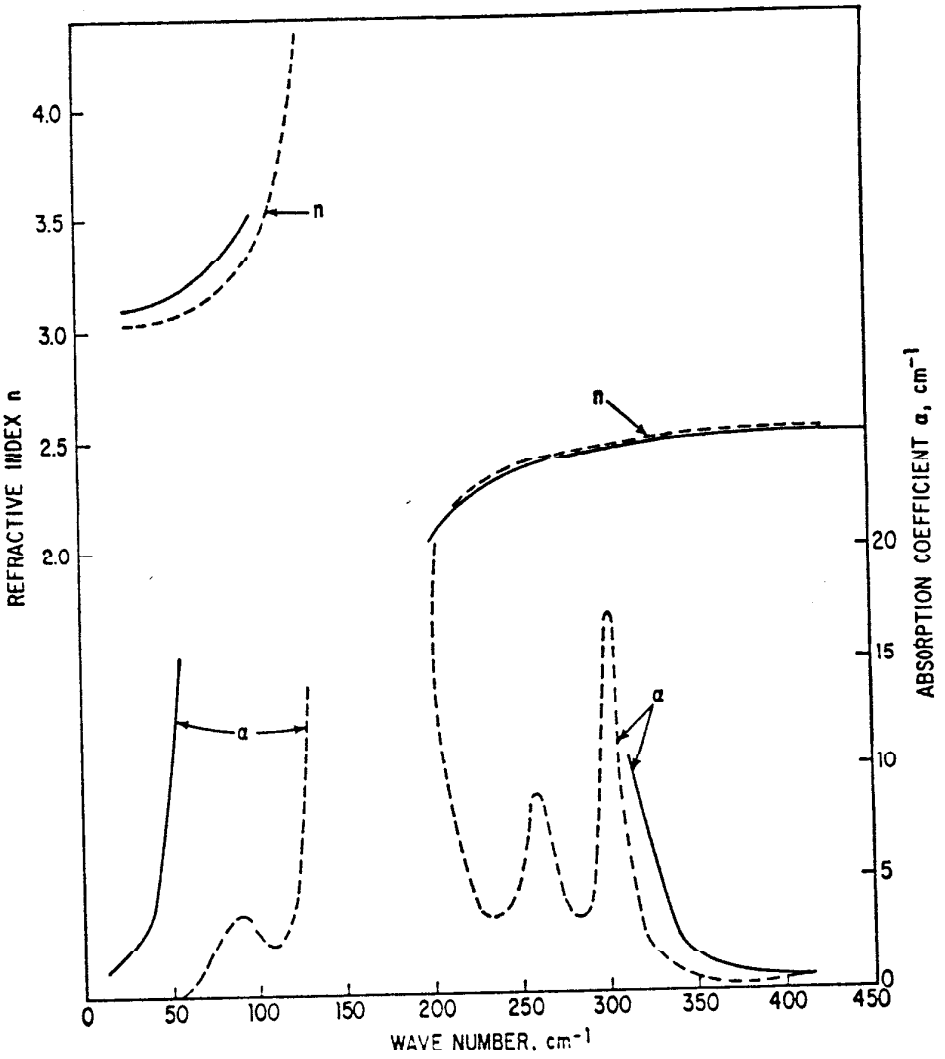

FIG. 6r-21. Optical constants of CdTe from 33 to 450 cm^{-1}. Solid line, 300 K; dashed line, 8 K. [*C. J. Johnson, G. H. Sherman, and R. Weil, Appl. Opt.* **8**, 1667 (1969).]

beam splitter at the Brewster angle (60 deg for Mylar) instead of the usual 45 deg, the interferometer produces 100 percent polarized radiation. The efficiency of a Mylar beam splitter 6 μm thick at 45 and 60 deg of angle incidence is illustrated in Fig. 6r-23.

The optical characteristics of a metal mesh depend upon λ/d, the ratio of wavelength to spacing. For $\lambda/d \gg 1$ the mesh acts as a mirror, whereas $\lambda/d \ll 1$ gives some transmission. The details of the reflection and transmission depend in a complicated way upon the details of the mesh geometry [2,3]. In the vicinity of $\lambda/d = 2$, however, the mesh acts as an acceptable beam splitter [4]. A variety of meshes are compared with a 12-μm Mylar beam splitter in Fig. 6r-24.

References for Sec. 6r-7

1. Loewenstein, E. V., and A. Engelsrath: *J. Phys. Suppl.* 3–4, **28**, 153 (1967).
2. Wessel, F.: *Hochfrequenztechnik* **54**, 62 (1939).
3. Ulrich, R.: *Infrared Phys.* **7**, 37 (1967).
4. Russell, E. E., and E. E. Bell: *Infrared Phys.* **6**, 75 (1966).

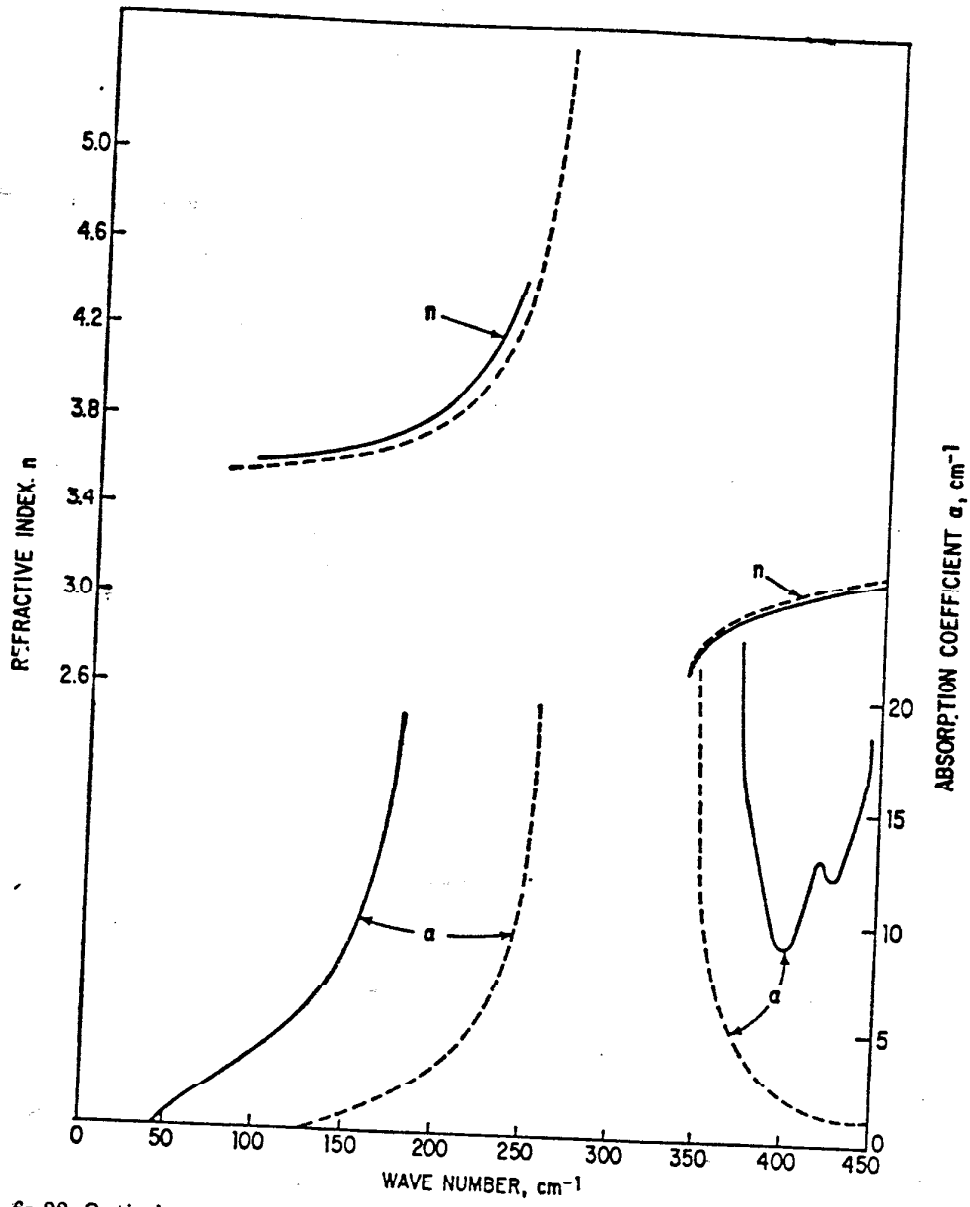

FIG. 6r-22. Optical constants of GaAs from 33 to 450 cm^{-1}. Solid line, 300 K; dashed line, 8 K. [*C. J. Johnson, G. H. Sherman, and R. Weil, Appl. Opt.* **8**, 1667 (1969).]

6r-8. Far-infrared Lasers. Listed in the following tables are the laser lines of wavelength greater than 50 μm reported through September, 1968. The power levels given are reported by most authors to be uncertain by a factor of 3. Even then, greater variations occur from one experimenter to another because the power depends on such factors as excitation conditions, gas pressure, and cleanliness of the discharge tube. The 337-μm line of HCN is the best example of the discrepancies to be found. In the pulsed mode it is reported in ref. 1 to produce 0.6-W peak, whereas ref. 19 reports 10-W peak power. In the continuous mode ref. 13 reports 0.1 W, whereas ref. 20 gives 0.6 W. All power levels listed in the tables are peak power in the pulsed mode except where specifically labeled otherwise.

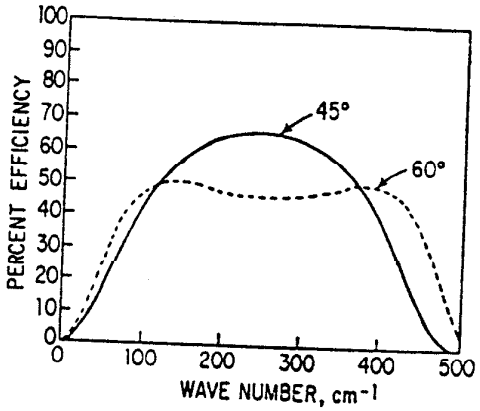

FIG. 6r-23. Calculated efficiency for Mylar beam splitters used at 45- and 60-deg angles of incidence. [*E. V. Loewenstein and A. Engelsrath, J. Phys. Suppl.* 3–4, **28**,153 (1967).]

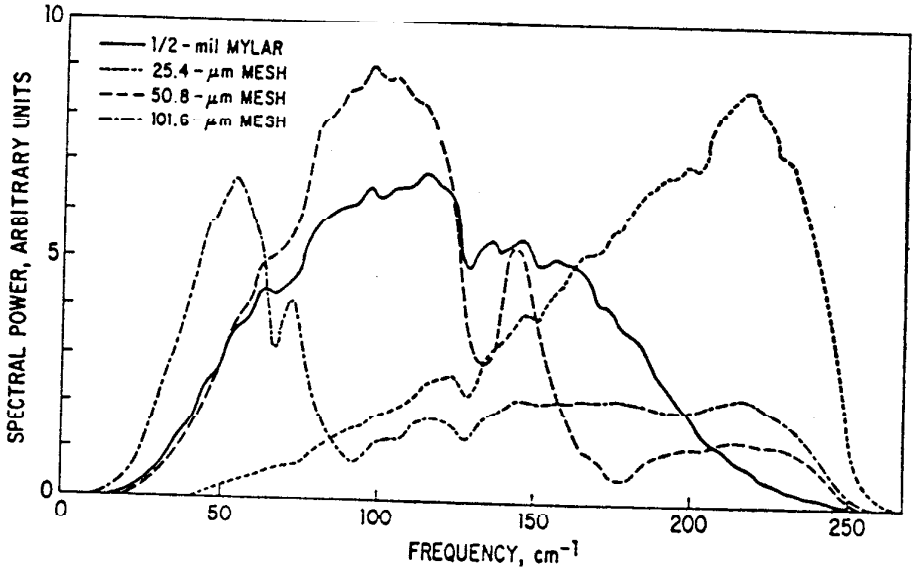

FIG. 6r-24. Background spectra obtained with various beam splitters under otherwise identical experimental conditions. [*E. E. Russell and E. E. Bell, Infrared Phys.* **6**, 75, (1966).]

Except in Table 6r-26 the wavelengths are the measured quantities, and the wave numbers given are simply $\sigma = 10^4/\lambda$.

In Table 6r-26 the frequencies were measured by comparison with a klystron, and the wavelengths were calculated using $C = 2.997925 \times 10^8$m/sec.

TABLE 6r-22. LASER LINES OBSERVED IN GASES CONTAINING N, C, AND H OR D

λ, μm	σ, cm⁻¹	Peak power, W	Assignment	Refs.
Dimethylamine, and Other Gases Containing C, H, and N				
71.899	139.084	0.3		1
73.101	136.796	0.008		
76.093	131.418	0.005		
77.001	129.868	0.003		
81.554	122.618	0.1		
96.401	103.733	0.2		
98.693	101.325	0.8		
101.257	98.759	0.2		
112.066	89.233	0.2		
116.132	86.109	0.5		
126.164	79.262	3		
128.629(CW)	77.743	9	$(12^{2d}0)27 \rightarrow (05^{1d}0)26$ $(12^{2d}0)26 \rightarrow (05^{1d}0)25$ $(12^{0}0)26 \rightarrow (05^{1c}0)25$ $(12^{0}0)26 \rightarrow (05^{1c}0)24$ } HCN	14
130.838	76.430	4		
134.932	74.111	0.8		
201.059	49.737	0.05		
211.001(CW)	47.393	0.2		
222.949	44.853	0.08		
309.731	32.2861	0.4		
310.908(CW)	32.1639	1	$(11'0)11 \rightarrow 10$ $(11'0)11 \rightarrow (04^{0}0)$ $(11'0)10 \rightarrow (04^{0}0)9$ $(04^{0}0)9 \rightarrow 8$ } HCN	2
336.579(CW)	29.7107	0.6		
372.547	26.8422	0.6		
537.7	18.60			11
538.2	18.58			
CH_3CN				
334.4	29.90			18
334.8	29.87			
CH_4 and $^{15}NH_3$				
110.240	90.711			1
113.311	88.253			
138.768	72.063			
165.150	60.551			
$CD_4 + ND_3$				
181.789	55.009	2×10^{-4}	$(22^{0}0)23 \rightarrow (22^{0}0)22$ $(22^{0}0)22 \rightarrow (09^{1c}0)21$ $(22^{0}0)21 \rightarrow (09^{1c}0)20$ $(09^{1c}0)20 \rightarrow (09^{1c}0)19$ } DCN	1, 8, and 14
189.948(CW)	52.646	3×10^{-4}		
194.706(CW)	51.359			
204.387	48.927			

TABLE 6r-23. LASER LINES OBSERVED IN H_2O AND D_2O

λ, μm	σ, cm^{-1}	Peak power, W	Assignment	Refs.
		H_2O		
53.906	185.51	0.0008		3
55.077(CW)	181.56	0.06	$(020)5_{50} \rightarrow (020)5_{41}$	4, 5, 6
57.660	173.43	0.02	$(100)9_{19} \rightarrow (020)8_{44}$	
67.177	148.86	0.01	$(100)6_{25} \rightarrow (020)5_{50}$; $(020)4_{41} \rightarrow (020)4_{32}$	
73.402	136.24	0.002		
78.455(CW)	127.46	0.007	$(100)8_{08} \rightarrow (020)8_{35}$	
79.106(CW)	126.41	0.006	$(020)8_{44} \rightarrow (020)8_{35}$	
89.775	111.39	0.006		
115.32(CW)	86.64	0.0007	$(020)8_{35} \rightarrow (020)8_{26}$	
118.65(CW)	84.28	0.001	$(001)6_{42} \rightarrow (020)6_{61}$	
120.08	83.28	.....	$(001)6_{42} \rightarrow (001)6_{33}$	
220.23(CW)	45.407	.....	$(100)5_{23} \rightarrow (020)5_{50}$	8
		D_2O		
56.845	175.92			3
71.965	138.96			
72.429	138.07			
72.747	137.46			
73.337	136.36			
74.545	134.15			
76.305	131.05			
84.111	118.89			
84.291(CW)	118.64			7
107.71(CW)	92.84			

TABLE 6r-24. LASER LINES OBSERVED IN NEON

λ, μm	σ, cm^{-1}	Continuous power, W	Assignment	Ref.
50.70(CW)	197.2		$7p[3/2]_2 - 6d[3/2]_2^0$	9
52.39(CW)	190.9		$7p'[1/2]_1 - 6d'[3/2]_2^0$	
55.68(CW)	179.6		$7p[3/2]_1 - 6d[7/2]_4^0$	
72.15(CW)	138.6		$8p'[1/2]_0 - 7d'[3/2]_1^0$	
86.9(CW)	115.1		$8p'[3/2]_2 - 7d'[5/2]_2^0$	
88.46(CW)	113.0	$>10^{-9}$	$8p[3/2]_1 - 7d[5/2]_2^0$	
89.93(CW)	111.20		$8p[5/2]_3 - 7d[7/2]_3^0$	
93.02(CW)	107.50			
106.02(CW)	94.322	$\sim 10^{-9}$	$10p[1/2]_0 - 9d[3/2]_1^0$	
124.4(CW)	80.39	$\sim 10^{-9}$	$9p[3/2]_1 - 8d[5/2]_2^0$	
126.1(CW)	79.30	$\sim 10^{-9}$	$9p[3/2]_2 - 8d[5/2]_3^0$	
132.8(CW)	75.30	$\sim 10^{-9}$		

TABLE 6r-25. LASER LINES OBSERVED IN MISCELLANEOUS GASES

Gas	λ, μm	σ, cm^{-1}	Peak power, W	Assignment	Ref.
ICN	773.5	12.928	3	$3p^1P_1^0 - 3d^1D_2$	12
He	95.788	109.94			10
CH_3CN and $(CH_3)_2SO_4$	119.0	84.0			18

TABLE 6r-26. LASER LINES WHOSE FREQUENCIES HAVE BEEN DETERMINED BY DIRECT COMPARISON WITH A KLYSTRON
(The wavelengths are calculated using $C = 2.997925 \times 10^8$ m/sec.)

Gas	Frequency, GHz	λ, μm	σ, cm^{-1}	Ref.
DCN	1,466.787	204.3872	48.92674	15
	1,539.257	194.7644	51.34409	
	1,539.745	194.7027	51.36035	
	1,577.789	190.0080	52.62937	
	1,578.279	189.9490	52.64571	
D_2O	1,578.279	189.9490	52.64571	16
C_2N_2	1,539.756	194.7013	51.36072	16
HCN	964.3123	310.8874	32.16599	17
	890.7595	336.5583	29.71253	

References for Sec. 6r-8

1. Mathias, L. E. S., A. Crocker, and M. S. Wills: *IEEE J. Quantum Electron.* QE-4, 205 (1968).
2. Lide, D. R., Jr., and A. G. Maki: *Appl. Phys. Letters* **11**, 62 (1967).
3. Mathias, L. E. S., and A. Crocker: *Phys. Letters* **13**, 35 (1964).
4. Hartman, B., and B. Kleman: *Appl. Phys. Letters* **12**, 168 (1968).
5. Benedict, W. S.: *Appl. Phys. Letters* **12**, 170 (1968).
6. Pollack, M. A., and W. J. Tomlinson: *Appl. Phys. Letters* **12**, 173 (1968).
7. Müller, W. M. and G. T. Flesher: *Appl. Phys. Letters* **8**, 217 (1966).
8. Müller, W. M., and G. T. Flesher: *Appl. Phys. Letters* **10**, 93 (1967).
9. Patel, C. K. N., W. L. Faust, R. A. McFarlane, and C. G. B. Garrett: *Proc. IEEE* **52**, 713 (1964).
10. Mathias, L. E. S., A. Crocker, and M. S. Wills: *IEEE, J. Quantum Electron.* QE-3, 170 (1967).
11. Steffen, H., J. Steffen, J. F. Moser, and F. K. Kneubühl: *Phys. Letters* **20**, 20 (1966).
12. Steffen, H., J. Steffen, J. F. Moser and F. K. Kneubühl: *Phys. Letters* **21**, 425 (1966).
13. Gebbie, H. A., N. W. B. Stone, W. Slough, J. E. Chamberlain, and W. A. Sheraton: *Nature* **211**, 62 (1966).
14. Maki, Arthur G.: *Appl. Phys. Letters* **12**, 122 (1968).
15. Hocker, L. O., and A. Javan: *Appl. Phys. Letters* **12**, 124 (1968).
16. Hocker, L. O., D. Ramachandra Rao, and A. Javan: *Phys. Letters* **24A**, 690 (1967).
17. Hocker, L. O., A. Javan, D. Ramachandra Rao, L. Frenkel, and T. Sullivan: *Appl. Phys. Letters* **10**, 147 (1967).
18. Prettl, W., and L. Genzel: *Phys. Letters* **23**, 443 (1966).
19. Gebbie, H. A., N. W. B. Stone, and F. D. Findlay, *Nature* **202**, 685 (1961).
20. Kotthaus, J. P.: *Appl. Opt.* **7**, 2422 (1968).